

行政院國家科學委員會專題研究計畫 成果報告

子計劃二：智慧型天線及多用戶偵測(I)

計畫類別：整合型計畫

計畫編號：NSC91-2219-E-009-024-

執行期間：91年08月01日至92年07月31日

執行單位：國立交通大學電信工程學系

計畫主持人：李大嵩

報告類型：完整報告

報告附件：出席國際會議研究心得報告及發表論文

處理方式：本計畫可公開查詢

中 華 民 國 92 年 10 月 27 日

政院國家科學委員會補助專題研究計畫

成果報告
期中進度報告

前瞻性 B3G 無線接取技術-子計畫二:智慧型天線及多用戶偵測(I)

Advanced Technologies for B3G Radio Access: Advanced Smart

Antennas and Multiuser Detection for B3G Radio Access

計畫類別： 個別型計畫 整合型計畫

計畫編號：NSC 91-2219-E-009-024

執行期間：九十一年八月一日至九十二年七月三十一日

計畫主持人：李大嵩 教授 交通大學電信系

共同主持人：

計畫參與人員：林高洲、鄧俊宏、何從廉、曹佑瑞、謝宜達、王建中

成果報告類型(依經費核定清單規定繳交)： 精簡報告 完整報告

本成果報告包括以下應繳交之附件：

赴國外出差或研習心得報告一份

赴大陸地區出差或研習心得報告一份

出席國際學術會議心得報告及發表之論文各一份

國際合作研究計畫國外研究報告書一份

處理方式：除產學合作研究計畫、提升產業技術及人才培育研究計畫、

列管計畫及下列情形者外，得立即公開查詢

涉及專利或其他智慧財產權， 一年 二年後可公開查詢

執行單位：國立交通大學電信工程系

中 華 民 國 九 十 二 年 十 月 二 十 七 日

Table of Contents

1. Abstract	1
2. Project Objectives	2
3. Project Methods and Achievements	3
3.1 Space Time Data Model	3
3.2 Linear Space Time RAKE Receiver	6
3.2.1 Construction of Adaptive Filters	6
3.2.2 Construction of Adaptive Beamformers and RAKE Receiver	8
3.2.3 Algorithm Summary	9
3.2.4 Implementation Issues	9
3.3 Development of Partially Adaptive ST CDMA Receiver	12
3.3.1 Construction of Blind Adaptive GSC Correction	12
3.3.2 Partially Adaptive Implementation Based on Krylov Subspace Technique	14
3.3.3 Partially Adaptive Implementation Based on Conjugate Gradient Method	16
3.3.4 RAKE Combining and Decision Aided Symbol Detection	18
3.4 Extended Research Achievement	20
4. Simulation Results	21
5. Conclusion	25
6. References	26

1. Abstract

Keyword: radio access, smart antenna, multiuser detection (MUD), beyond 3G wireless communications

With the fast development of personal communications and increasing need of multi-media messaging, the frequency spectrum becomes more and more a precious resource. As a result, the major topic for future B3G wireless communications will be to effectively enhance the capability of radio access to provide excellent spectral efficiency and system capacity, so that high data rate transmission and multi-media services can be realized. To these ends, several schemes shall be developed, among which the smart antenna and multiuser detection (MUD) techniques would be the most significant research topics. The main reason why the two techniques have received much attention in B3G wireless communications is that they can suppress interference effectively (including multiple access interference and cochannel interference) without the need of extra spectra. This would help to increase the transmission capacity of the system. They can also provide the spatial diversity to overcome channel fading and enhance reliability of signal reception. In this project, we will study the feasibility of smart antenna and MUD techniques applied to B3G wireless communications.

In this project, we had thoroughly studied the smart antenna and multiuser detection algorithms. Significant results had been achieved. We had proposed the 'Linear space-time RAKE receiver', 'Multi-antenna Low Complexity Partially Adaptive Interference Canceller Based on Krylov subspace technique' and 'Multi-antenna Partially Adaptive Interference Canceller Based on Conjugate Gradient Method'. We had also proposed a transceiver architecture for MIMO MC-CDMA for high data rate applications based on interactions with other cooperating projects.

2. Project Objectives

In wideband CDMA systems, the multipath environment can be exploited through the RAKE receiver, allowing signals arriving at the receiver with different propagation delays to be independently received and coherently combined by exploiting the temporal signature of the channel. On the other hand, in order to successfully detect data from the desired user, the MAI need to be suppressed effectively. Adaptive multi-user detectors (MUD) and interference cancellers have been suggested which provide full or partial immunity to the near-far effect [1]. The performance of an optimal MUD [1] in a multi-user system can approach that in a single-user environment. Unfortunately, the optimal MUD is impractically complex. As an alternative, the sub-optimal linear multi-user detector is an improved version of the conventional RAKE receiver, with the improvement due to better MAI suppression via either post- or pre-despread processing. The post-despread MUD works with the outputs of a bank of filters, each matched to a user of interest. The pre-despread MUD can be regarded as an adaptive matched filter that performs despreading and MAI suppression simultaneously. Popular pre-despread MUD's include the minimum mean squared error (MMSE) [3] and minimum output energy (MOE) receivers [4]. In particular, the MOE receiver derives its filter weights by minimizing the output energy subject to a unit response constraint for the desired signal. It is similar in structure to the linearly constrained minimum variance (LCMV) beamformer in array processing and is shown to offer the performance of the MMSE receiver without the need of channel information. Unfortunately, the MOE receiver exhibits high sensitivity to channel mismatch and does not perform reliably in the presence of multipath propagation. Although the pre-despread CDMA receivers provide excellent MAI suppression, they require a high dimension adaptive processing. To reduce the complexity, partially adaptive (PA) realization is suggested as an alternative with which the number of adaptive weights is reduced [5]-[7]. The advantages of PA implementation include not only reduced complexity but also faster convergence. In this project, three space-time (ST) CDMA receivers with enhanced interference suppression are proposed for pilot symbols assisted wireless systems. Among them, two are based on PA techniques to reduce system computational load.

3. Project Methods and Achievements

In this project, we had proposed three ST CDMA receivers, including

- (1) Linear space-time RAKE receiver
- (2) Multi-antenna low complexity partially adaptive interference canceller based on Krylov subspace technique
- (3) Multi-antenna partially adaptive interference canceller based on conjugate gradient (CG) Method

The detailed design procedures are discussed in the following sections.

3.1 Space Time Data Model

Consider the uplink CDMA data model for a scenario in which the receiver of basestation is equipped with an antenna array of N_r elements. Figure 1 shows the configuration of a linear equally spaced antenna array in which the spacing between two neighboring antennas is set to half wavelength. Assuming that each transmitter is equipped with a single antenna, the baseband multipath channel between the k th user's transmitter and the baseband receiver can be modeled as a single input multiple output (SIMO) system. To develop the SIMO data model, firstly the complex baseband lowpass equivalent transmitted signal $r_k(t)$ of the k th user during the i th data symbol is defined as

$$r_k(t) = \sigma_k \sum_i d_k(i) c_k(t - iT) \quad (1)$$

where $d_k(i)$ denotes the i th transmitted information symbol assumed to be i.i.d. with zero-mean and unit variance, T is the symbol duration, σ_k^2 is the transmit power, and $c_k(t)$ is the signature waveform given by

$$c_k(t) = \sum_{m=0}^{M-1} c_k[m] p(t - mT_c) \quad (2)$$

where $c_k[m]$ is the spreading sequence of the k th user, M is the spreading factor, $p(t)$ is the chip waveform, and T_c is the chip duration. Putting the K user signals together, the received baseband data at the n_r th receive antenna can be expressed in the following form:

$$x^{(n_r)}(t) = \sum_{k=1}^K \sigma_k \sum_{l=1}^L \alpha_{n_r,k,l} r_k(t - \tau_{k,l}) + i_{NB}(i) + n(t) \quad (3)$$

where $i_{NB}(i)$ denotes narrowband interference, and $\tau_{k,l}$ and $\alpha_{n_r,k,l}$ are the delay and complex gain, respectively, of the l th path of the k th user, and $n(t)$ is the additive white noise

process with power σ_n^2 . It is assumed that the L paths arrive within a delay spread of L chips, with each path having a different delay of integer number of chips. It is also assumed that initial acquisition is performed properly such that a rough estimate of timing offset is available for each user. To fully exploit the temporal signature, $x^{(n_r)}(t)$ is chip matched filtered and then chip rate sampled at $t = iT_s + mT_c$ over one symbol duration plus delay spread, i.e., $m = 0, 1, \dots, M + L - 2$. The resulting discrete-time data over the i th symbol is given by

$$x_m^{(n_r)}(i) = \sum_{k=1}^K \sigma_k \sum_{l=1}^L \alpha_{n_r, k, l} r_{k, m}(i) + i_{NB, m}(i) + n_m(i) \quad (4)$$

where

$$r_{k, m}(i) = r_k(iT_s + mT_c - \tau_{k, l}) \quad (5)$$

$$i_{NB, m}(i) = i_{NB}(iT_s + mT_c) \quad (6)$$

$$n_m(i) = n(iT_s + mT_c) \quad (7)$$

Assuming that the user 1 is the desired user, and putting the chip-sampled data over the i th symbol into an $(M + L - 1) \times 1$ vector, we have

$$\begin{aligned} \mathbf{x}^{(n_r)}(i) &= [x_0^{(n_r)}(i), x_1^{(n_r)}(i), \dots, x_{M+L-2}^{(n_r)}(i)] \\ &= \sum_{k=1}^K \sigma_k \sum_{l=1}^L \alpha_{n_r, k, l} \mathbf{c}_{k, l} d_k(i) + \mathbf{i}_{NB}^{(n_r)}(i) + \mathbf{n}^{(n_r)}(i) \\ &= \mathbf{h}_1^{(n_r)} d_1(i) + \sum_{k=2}^K \mathbf{h}_k^{(n_r)} d_k(i) + \mathbf{i}_{NB}^{(n_r)}(i) + \mathbf{n}^{(n_r)}(i) \\ &= \mathbf{s}_1^{(n_r)}(i) + \mathbf{i}^{(n_r)}(i) + \mathbf{n}^{(n_r)}(i) \end{aligned} \quad (8)$$

where \mathbf{T} denotes the transpose,

$$\mathbf{c}_{k, l} = [\mathbf{0}_{l-1}^T, c[0], c[1], \dots, c[M-1], \mathbf{0}_{L-l}^T]^T \quad (9)$$

and $\mathbf{0}_n$ is the $n \times 1$ zero vector. The $\mathbf{h}_k^{(n_r)}$ is the effective composite signature vector (CSV) of user k at the n_r th receive antenna given by:

$$\mathbf{h}_k^{(n_r)} = \sigma_k \sum_{l=1}^L \alpha_{n_r, k, l} \mathbf{c}_{k, l} \quad (10)$$

Finally, $\mathbf{i}^{(n_r)}(i) = \sum_{k=2}^K \mathbf{h}_k^{(n_r)} d_k(i) + \mathbf{i}_{NB}^{(n_r)}(i)$ is the vector consisting of MAI and NBI, and $\mathbf{n}^{(n_r)}(i)$ is the noise vector.

Stacking the data vectors $\mathbf{x}^{(1)}(i), \dots, \mathbf{x}^{(N_r)}(i)$, we have

$$\begin{aligned} \mathbf{x}(i) &= \left[\mathbf{x}^{(1)T}(i) \ \mathbf{x}^{(2)T}(i) \ \dots \ \mathbf{x}^{(N_r)T}(i) \right]^T \\ &= \mathbf{h}_1 d_1(i) + \mathbf{i}(i) + \mathbf{n}(i) \end{aligned} \quad (11)$$

where

$$\mathbf{h}_1 = \left[\mathbf{h}_1^{(1)T} \quad \mathbf{h}_1^{(2)T} \quad \dots \quad \mathbf{h}_1^{(N_r)T} \right]^T \quad (12)$$

$$\mathbf{i}(i) = \left[\mathbf{i}^{(1)T}(i) \quad \mathbf{i}^{(2)T}(i) \quad \dots \quad \mathbf{i}^{(N_r)T}(i) \right]^T \quad (13)$$

$$\mathbf{n}(i) = \left[\mathbf{n}^{(1)T}(i) \quad \mathbf{n}^{(2)T}(i) \quad \dots \quad \mathbf{n}^{(N_r)T}(i) \right]^T \quad (14)$$

A receiver for user 1 is designed to identify \mathbf{h}_1 to retrieve $d_1(i)$ from $\mathbf{i}(i)$ and $\mathbf{n}(i)$. In particular, a linear receiver combines $\mathbf{x}(i)$ using a weight vector \mathbf{w} to obtain

$$z_1(i) = \mathbf{w}_1^H \mathbf{x}(i) \quad (15)$$

where H denotes the complex conjugate transpose. A popular criteria for choosing \mathbf{w}_1 leads to the MMSE receiver:

$$\mathbf{w}_{MMSE} = \mathbf{R}_x^{-1} \hat{\mathbf{h}}_1 \quad (16)$$

where $\hat{\mathbf{h}}_1$ is an estimate of \mathbf{h}_1 and \mathbf{R}_x is the data correlation matrix given by

$$\mathbf{R}_x = E\{\mathbf{x}(i)\mathbf{x}^H(i)\} = \mathbf{R}_s + \mathbf{R}_{in} \quad (17)$$

where

$$\mathbf{R}_s = E\{\mathbf{s}_1(i)\mathbf{s}_1^H(i)\} \quad (18)$$

$$\mathbf{R}_{in} = E\{(\mathbf{i}(i) + \mathbf{n}(i))(\mathbf{i}(i) + \mathbf{n}(i))^H\} \quad (19)$$

Another type of optimal receiver is the maximum SINR (MSINR) receiver given by

$$\mathbf{w}_{MSINR} = \mathbf{R}_{in}^{-1} \hat{\mathbf{h}}_1 \quad (20)$$

However, \mathbf{R}_{in} is not available in practice, and is usually estimated by decision aided schemes.

Finally, the symbol decision $\hat{d}_1(i)$ can be obtained by

$$\hat{d}_1 = \text{dec}\{z_1\} \quad (21)$$

3.2 Linear Space Time RAKE Receiver

A CDMA ST RAKE receiver suitable for pilot symbol assisted systems is developed with a three-stage procedure. First, a set of L adaptive filters is constructed at each of the N_r antennas to perform diversity reception of the multipath signal and MAI suppression blindly. In particular, these LN_r adaptive filters are realized in a modified form of generalized sidelobe canceller (GSC) to avoid the signal cancellation phenomenon incurred with channel mismatch. Second, a set of L adaptive beamformers is constructed, one for each finger, which provides effective suppression of time-varying NBI, which minimizes the mean square error between the beamformer output and a reference signal (pilot symbols or tentative detected data symbols). These beamformers are realized according to the MMSE criterion with the aid of pilot symbols. Finally, beamformer outputs from different fingers are RAKE combined to capture the multipath signal coherently. This leads to a CDMA ST RAKE receiver. The advantages of working with the GSC blind adaptive filters are twofold. First, blind adaptive filters can perform signal reception and MAI suppression without the need of pilot symbols assisted channel estimation, which cannot be done reliably in the presence of strong interference. Moreover, they can utilize the entire received data symbols, rather than just the pilot symbols, to compute the adaptive weights, leading to improved performance. Second, the GSC can alleviate the signal cancellation phenomenon often occurring in the LCMV algorithms, which means that the signal may be treated as interference and gets cancelled if the channel is not known exactly. A modified GSC is proposed in which the multipath signal is removed in the lower branch by a pre-designed blocking matrix before adaptive processing, such that MAI suppression can be done blindly without the need of channel information. With the preprocessing offered by adaptive filters, MAI can be greatly reduced, leading to a significant improvement in the subsequent beamforming and RAKE combining. The overall schematic diagram of the proposed receiver is depicted in Figure 2.

3.2.1 Construction of Adaptive Filters

In temporal processing, it is convenient to treat the signature vector $\mathbf{c}_{1,l}$ as a steering vector. In this way, an adaptive filter is simply a time domain analogy of a beamformer, and

the beamforming concept can be readily applied. According to this, the adaptive filter output data is

$$y_{1,l}^{(n_r)}(i) = \mathbf{f}_{1,l}^{(n_r)H} \mathbf{x}^{(n_r)}(i) \quad (22)$$

where $\mathbf{f}_{1,l}^{(n_r)}$ is the adaptive filter weight vector for the l th finger of user 1 at the n_r th antenna, and is the $(M + L - 1) \times 1$ data vector received by the antenna.

To ensure an effective suppression of MAI, adaptive cancellation is performed for each of the adaptive filters. This is done by choosing the filter weight vectors in accordance with the LCMV criterion [5], [6], [8], [9]:

$$\begin{aligned} \min_{\mathbf{w}_{1,l}^{(n_r)}} & \mathbf{f}_{1,l}^{(n_r)H} \mathbf{R}_x \mathbf{f}_{1,l}^{(n_r)} \\ \text{subject to:} & \mathbf{f}_{1,l}^{(n_r)H} \mathbf{c}_{1,l} = 1 \end{aligned} \quad (23)$$

for $l = 1, K, L$ and $j = 1, K, N_r$, where

$$\mathbf{R}_x^{(n_r)} = E\{\mathbf{x}^{(n_r)}(i)\mathbf{x}^{(n_r)H}(i)\} \quad (24)$$

is the data correlation matrix at the n_r th antenna. A major problem of the LCMV algorithm is the phenomenon of signal cancellation due to the mismatch of signature vectors. This means that the filter tends to treat the signal as interference and cancel it in order to minimize the output power. The concept of GSC is to decompose the weight vector into two orthogonal components: $\mathbf{f}_{1,l}^{(n_r)} = \mathbf{c}_{1,l} - \mathbf{B}\mathbf{u}_{1,l}^{(n_r)}$. Different from the conventional GSC in which the blocking matrix would be designed to remove the signal at a single finger, a modified form of GSC is proposed in which the blocking matrix is designed to remove all the multipath signal components. This is essential since if the signal is not entirely removed in the lower branch, a mutual cancellation of the signal will occur between the upper and lower branches of the GSC. Following the standard procedure of GSC, the adaptive weight vectors are determined by the following MMSE problem:

$$\min_{\mathbf{u}_{1,l}^{(n_r)}} [\mathbf{c}_{1,l} - \mathbf{B}\mathbf{u}_{1,l}^{(n_r)}]^H \mathbf{R}_x^{(n_r)} [\mathbf{c}_{1,l} - \mathbf{B}\mathbf{u}_{1,l}^{(n_r)}] \quad (25)$$

Solving for $\mathbf{u}_{1,l}^{(n_r)}$ and substituting in $\mathbf{f}_{1,l}^{(n_r)}$ yields

$$\mathbf{f}_{1,l}^{(n_r)} = [\mathbf{I} - \mathbf{B}(\mathbf{B}^H \mathbf{R}_x^{(n_r)} \mathbf{B})^{-1} \mathbf{B}^H \mathbf{R}_x^{(n_r)}] \mathbf{c}_{1,l} \quad (26)$$

Note that \mathbf{B} is shared by all the $L_1 N_r$ filters and chosen to be a full rank $M \times (M - L_1)$

matrix whose columns are orthogonal to the set of signature vectors $\mathbf{C}_1 = [\mathbf{c}_{1,1}, \mathbf{c}_{1,2}, \dots, \mathbf{c}_{1,L}]$, i.e., a solution to the equation $\mathbf{B}^H \mathbf{C}_1 = \mathbf{O}$, where $\mathbf{c}_{1,l}$ is given by (9).

3.2.2 Construction of Adaptive Beamformers and RAKE Receiver

With a sufficiently large degrees-of-freedom, the MAI can be suppressed effectively by the adaptive filters. Unfortunately, they may not be able to suppress time varying NBI whose signatures change from one symbol to another. As described in [10] and [11], an NBI can be treated as an MAI with a time-varying signature vector, or a set of many MAI's with a fixed signature vector. Since a degree-of-freedom is required to suppress a stationary MAI, the adaptive filters cannot effectively suppress the NBI with their limited degrees-of-freedom. However, NBI's can be suppressed in the spatial domain by adaptive beamforming as long as their AOA's are separated from that of signal-of-interest, and are slowly varying relative to the processing speed of the receiver. In the following, a pilot symbols assisted adaptive beamformer based on the MMSE criterion is constructed for each finger. First, the adaptive filter outputs $y_{1,l}^{(n_r)}$, $l = 1, K, N_r$, at the N_r antennas for the l th finger are weighted and summed to produce the beamformer output:

$$z_{1,l}(i) = \mathbf{w}_{1,l}^H \mathbf{y}_{1,l} \quad (27)$$

where

$$\mathbf{y}_{1,l}(i) = [y_{1,l}^{(1)}(i), y_{1,l}^{(2)}(i), \dots, y_{1,l}^{(N_r)}(i)]^T \quad (28)$$

with $\mathbf{w}_{1,l}^{(n_r)}$'s being the beamforming weight vectors for the l th finger. The weight vector $\mathbf{w}_{1,l}$ is determined in accordance with the MMSE criterion:

$$\min_{\mathbf{w}_{1,l}} E\{|\mathbf{w}_{1,l}^H \mathbf{y}_{1,l}(i) - d_1(i)|^2\} \quad (29)$$

where $d_1(i)$ is the pilot symbol sequence. The solution is given by

$$\mathbf{w}_{1,l} = \mathbf{R}_{1,l}^{-1} \mathbf{r}_{1,l} \quad (30)$$

where

$$\mathbf{R}_{1,l} = E\{\mathbf{y}_{1,l}(i) \mathbf{y}_{1,l}^H(i)\} \quad (31)$$

is the post-despread data correlation matrix, and

$$\mathbf{r}_{1,l} = E\{\mathbf{y}_{1,l}(i) d_1^*(i)\} \quad (32)$$

The final stage of the receiver is to combine the beamformer outputs $z_{1,l}(i)$, $l = 1, K, L$, at the

L fingers in a coherent manner in order to fully utilize the multipath energy. Since the channel effects have been compensated for by the beamforming weight vectors $\mathbf{w}_{1,l}$'s, the output of the RAKE receiver is simply obtained as

$$z_1(i) = \sum_{l=1}^{L_1} \mathbf{w}_{1,l}^H \mathbf{y}_{1,l}(i) \quad (33)$$

which is then sent to the data decision device:

$$\hat{d}_1(i) = \text{dec}\{z_1(i)\} \quad (34)$$

3.2.3 Algorithm Summary

In practice, the data correlation matrices are usually estimated by the sample average versions:

$$\mathbf{R}_x \approx \frac{1}{N_s} \sum_{i=1}^{N_s} \mathbf{x}(i) \mathbf{x}^H(i) \quad (35)$$

$$\mathbf{R}_x^{(n_r)} \approx \frac{1}{N_s} \sum_{i=1}^{N_s} \mathbf{x}^{(n_r)}(i) \mathbf{x}^{(n_r)H}(i) \quad (36)$$

$$\mathbf{R}_{1,l} = \frac{1}{N_s} \sum_{i=1}^{N_s} \mathbf{y}_{1,l}(i) \mathbf{y}_{1,l}^H(i) \quad (37)$$

where N_s is the number of symbols used for the processing period.

The information required in the proposed receiver is the spreading code and timing of the signal-of-interest so that the GSC blocking matrix \mathbf{B} can be determined beforehand.

Algorithm summary of the proposed ST CDMA receiver is as follows:

1. Compute in parallel $\mathbf{f}_{1,l}^{(n_r)}$, $l=1, \mathbf{K}, L$, $j=1, \mathbf{K}, N_r$, according to (26), with $\mathbf{R}_x^{(n_r)}$ estimated by (36) and \mathbf{B} determined by $\mathbf{B}^H \mathbf{c}_{1,l} = \mathbf{0}$, $l=1, \mathbf{K}, L$.
2. Compute in parallel $\mathbf{w}_{1,l}$, $l=1, \mathbf{K}, L$, according to (30), with $\mathbf{R}_{1,l}$ estimated by (37).
3. Obtain $z_{1,l}(i)$ according to (27).
4. Obtain $z_1(i)$ according to (33).

3.2.4 Implementation Issues

(a) Numerical Stability

In the direct matrix inversion implementation, the computation of temporal adaptive weight

vector $\mathbf{f}_{1,l}^{(n_r)}$ in (26) involves the inversion of $\mathbf{R}_x^{(n_r)}$. Numerical instability may arise when there are few strong interferences present, such that the eigenvalue spread of the data correlation matrix $\mathbf{R}_x^{(n_r)}$ is large [12]. In this case, $\mathbf{R}_x^{(n_r)}$ will be ill conditioned and the matrix inversion in (26) will be numerically unstable, which means that a small error in $\mathbf{R}_x^{(n_r)}$ (due to finite sample size) may leads to a large deviation in the weight vectors. On the other hand, the performance of the adaptive filters may be poor due to the residual signal not completely removed by the blocking matrix. In the presence of residual signal in the lower branch, the GSC will perform a certain degree of mutual cancellation of the signal, leading to poor output SINR. To remedy these, pseudo noise terms $\eta_u \mathbf{I}$ can be added to $\mathbf{R}_x^{(n_r)}$, i.e., $\mathbf{R}_x^{(n_r)} = \mathbf{R}_x^{(n_r)} + \eta_u \mathbf{I}$, to alleviate the sensitivity problem. The pseudo noise has the effect of deemphasizing the strong interference and masking the residual signal, and can help to improve signal reception. It should be chosen large enough to handle the ill-condition problem, but not too large to distort the original signal scenario. A suitable choice which proves effective is such that η_u is equal to a small fraction (e.g., 0.1-0.3) of the largest eigenvalue of $\mathbf{R}_x^{(n_r)}$ [13].

(b) Recursive computation of weight vector

For a more efficient and practical implementation, the GSC can be realized in a time-recursive fashion using stochastic gradient algorithms such as LMS. This leads to recursive formulation of the solutions to (25):

$$\mathbf{u}_{1,l}^{(n_r)}(i+1) = \mathbf{u}_{1,l}^{(n_r)}(i) + \mu_u [\mathbf{c}_{1,l}^H \mathbf{x}^{(n_r)}(i) - \mathbf{u}_{1,l}^{(n_r)H}(i) \mathbf{B} \mathbf{u}_{1,l}^{(n_r)}(i)]^* \mathbf{B}^H \mathbf{x}^{(n_r)}(i) \quad (38)$$

for $i=1,2,\mathcal{K}$, where μ_u is the step-size of adaptation. The recursive algorithm does not exhibit the numerical instability as the DMI algorithm since it does not involve a matrix inversion. It is shown that the convergence of blind recursive algorithms is slow and noisy compared to training signal based algorithms. In view of this drawback, it is suggested that the proposed GSC-based adaptive filters are operated in blind mode in the initialization stage. When the output SINR has been improved and reliable detection is achieved for the signal, the receiver can be switched to the pilot symbols aided or decision-directed mode for better

convergence and performance.

The weight vector $\mathbf{w}_{1,l}(i)$ in (27) can be also recursively updated according to the LMS algorithm:

$$\mathbf{w}_{1,l}(i+1) = \mathbf{w}_{1,l}(i) + \mu_w [\hat{d}_1(i) - \mathbf{w}_{1,l}^H(i) \mathbf{y}_{1,l}(i)]^* \mathbf{y}_{1,l}(i) \quad (39)$$

where μ_w is the step size, and $\hat{d}_1(i)$ is the pilot symbol sequence or the tentative data decisions (in decision directed mode if necessary).

3.3 Development of Partially Adaptive ST CDMA Receiver

In this section, an efficient pre-despread adaptive ST CDMA receiver is developed which offers the performance of the ST MMSE receiver. The receiver consists of a set of adaptive correlators and a RAKE combiner for exploiting path diversity. A decision aided scheme is included for performance enhancement. The schematic diagram of the receiver is depicted in Figure 3. The design of the receiver involves the following procedures. First, a set of adaptive correlators is constructed to collect multipath signals with different delays. The tap weights of each correlator are determined in accordance with the LCMV criterion so that strong MAI can be effectively suppressed blindly. To avoid signal cancellation incurred with channel mismatch, these LCMV correlators are realized in the form of GSC. For reduced complexity processing, partial adaptivity is incorporated, which is done by selecting a reduced dimension subspace of the column space of the blocking matrix by using the Krylov subspace and CG techniques. Second, a simple coherent RAKE combiner with pilot aided channel estimation gives the desired user's symbol decisions. Since strong interference has been removed, channel estimation can be done accurately with a small number of pilot symbols. Finally, further performance enhancement is achieved by an iterative scheme in which the signal is reconstructed and subtracted from the GSC correlators input, leading to faster convergence of the receiver. The proposed low complexity PA receivers are suitable for the uplink of wireless CDMA systems, and are shown to outperform the conventional fully adaptive MMSE receiver by using a relatively small number of pilot symbols.

3.3.1 Construction of Blind Adaptive GSC Correlators

A set of adaptive correlators is used to perform despreading and MAI suppression. They are realized in the form of GSC, and require no pilot symbols for channel estimation. In other words, these correlators are "blind" and can utilize the entire received symbols, including data and pilot, to compute the adaptive weights. This is in contrast to non-blind pilot aided methods (e.g., MMSE) which cannot achieve reliable channel estimation in the presence of strong MAI by using the limited number of pilot symbols.

In order to restore the processing gain and retain the path diversity, $\mathbf{x}(i)$ is despread

using a set of discrete-time correlators:

$$z_{1,l}(i) = \mathbf{w}_l^H \mathbf{x}(i) = \mathbf{w}_l^H \mathbf{h}_1 d_1(i) + \mathbf{w}_l^H \mathbf{i}(i) + \mathbf{w}_l^H \mathbf{n}(i) \quad (40)$$

or $l=1, K, L$, where \mathbf{w}_l is the correlator weight vector at the l th finger. For an effective suppression of MAI, these weight vectors can be determined in accordance with the LCMV criterion:

$$\min_{\mathbf{w}_l} \mathbf{w}_l^H \mathbf{R}_x \mathbf{w}_l \quad \text{subject to} \quad \mathbf{c}_{1,l}^H \mathbf{w}_l = 1 \quad (41)$$

However, the adverse phenomenon of signal cancellation usually occurs with the solution in (15) due to the mismatch of signature vectors (i.e., mismatch between $\mathbf{c}_{1,l}$ and \mathbf{h}_1). With such a mismatch present, the signal can be treated as interference and receive a very small gain. To avoid such signal cancellation, the LCMV correlators can be implemented with multiple constraints. Here an alternative solution is suggested based on the GSC technique. The GSC is essentially an indirect but simpler implementation of the LCMV receiver. It is a widely used structure that allows a constrained adaptive algorithm to be implemented in an unconstrained fashion [5], [6].

The concept of GSC, as depicted in Figure 4 (a), is to decompose the weight vector into two orthogonal components as $\mathbf{w}_l = \mathbf{c}_{1,l} - \mathbf{B}\mathbf{u}_l$. The matrix \mathbf{B} is a pre-designed signal "blocking matrix" which removes user 1's signal before filtering. The goal is then to choose the adaptive weight vector \mathbf{u}_l to cancel the interference in $\mathbf{x}(i)$. According to the GSC scheme, \mathbf{u}_l is determined via the MMSE criterion:

$$\min_{\mathbf{u}_l} \left\{ \left| \mathbf{c}_{1,l}^H \mathbf{x}(i) - \mathbf{u}_l^H \mathbf{B} \mathbf{x}(i) \right|^2 \right\} \quad (42)$$

Since the signal has been removed in the lower branch by \mathbf{B} , the only way to minimize the MSE is such that \mathbf{u}_l performs a mutual cancellation of the MAI between the upper and lower branches. Solving for \mathbf{u}_l and substituting in $\mathbf{w}_l = \mathbf{c}_{1,l} - \mathbf{B}\mathbf{u}_l$, we get

$$\mathbf{w}_l = \left[\mathbf{I} - \mathbf{B}(\mathbf{B}^H \mathbf{R}_x \mathbf{B})^{-1} \mathbf{B}^H \mathbf{R}_x \right] \mathbf{c}_{1,l} \quad (43)$$

This is called the direct-matrix-inversion (DMI) implementation of the fully adaptive (FA) GSC correlators. Note that \mathbf{B} must block signals from the entire delay spread in order to avoid signal cancellation. It can be chosen to be a full rank $[N_r(M+L-1)] \times [N_r(M-1) + L(N_r-1)]$ matrix whose columns are orthogonal to

$\{\mathbf{c}_{1,1}, \dots, \mathbf{c}_{1,L}\}$, i.e., $\mathbf{B}^H \mathbf{c}_{1,l} = \mathbf{0}$, $l=1, \dots, L$. The distortion of signature vectors $\mathbf{c}_{1,l}$'s is typically tolerable in signal blocking, i.e., the signal component can be reliably removed by the above designed \mathbf{B} .

In the DMI implementation, the computation of adaptive weight vectors in (43) involves the inversion of $\mathbf{B}^H \mathbf{R}_x \mathbf{B}$, which is $[N_r(M-1) + L(N_r-1)] \times [N_r(M-1) + L(N_r-1)]$. With a large M , this requires a high computational load and is likely to incur numerical instability and poor convergence behaviors. To alleviate this problem, the PA GSC is proposed which uses only a portion of the available degrees of freedom offered by the adaptive weights. Specifically, the PA techniques can be employed to reduce the size of \mathbf{B} or dimension of \mathbf{u}_l 's [5]-[7]. For example, the Cross-Spectral PA (CS-PA) technique is developed by working with a smaller blocking matrix constructed from a reduced-dimensional subspace of $\text{Range}(\mathbf{B})$ to provide the lowest MMSE [7], and requires complicated eigen-computation. In the following, a simple and effective PA technique is proposed which is suitable for the downlink of wireless communications.

3.3.2 Partially Adaptive Implementation Based on Krylov Subspace Technique

The PA GSC, as shown in Figure 4 (b), works with P ($P < N_r(M-1) + L(N_r-1)$) adaptive weights through the use of a $[N_r(M-1) + L(N_r-1)] \times P$ linear transformation \mathbf{T}_l for the l th finger. This leads to a reduced size blocking matrix $\mathbf{B}_l = \mathbf{B} \mathbf{T}_l$. The criteria for the selection of \mathbf{T}_l include: (i) \mathbf{B}_l should be as small as possible (ii) MAI should be retained as much as possible in the lower branch. Criterion (i) is for complexity reduction and (ii) is for optimal mutual cancellation of MAI in the upper and lower branches [14]. Criterion (ii) is equivalent to saying that a reduced size blocking matrix should be chosen such that the upper and lower branch outputs of the GSC have a large crosscorrelation. Since the lower branch contains no signal, the only way to maximize the crosscorrelation is to retain as much MAI as possible in the lower branch. By doing so, a maximum mutual cancellation of interference can be achieved between the upper and lower branches. In the following, an efficient method for finding \mathbf{B}_l 's is developed based on the Krylov subspace technique.

According to [15], a reliable reduced rank MMSE solution can be found by projecting the data vector $\mathbf{x}(i)$ onto a P -dimensional subspace represented by the Krylov subspace

span:

$$\tilde{\mathbf{x}}(i) = \mathbf{S}_P \mathbf{x}(i) \quad (44)$$

where $\mathbf{S}_P = \{\mathbf{H}_1, \mathbf{R}_x \mathbf{H}_1, \mathbf{K}, \mathbf{R}_x^{(P-1)} \mathbf{H}_1\}$ is the $N_r(M+L-1) \times P$ dimension reduction transformation. The reduced rank solution is then given by $\mathbf{w}_{MMSE} = (\mathbf{S}_P^H \mathbf{R}_x \mathbf{S}_P)^{-1} \mathbf{S}_P^H \mathbf{H}_1$. The same technique can be applied to the GSC problem by considering $\mathbf{B}^H \mathbf{x}(i)$ as the data vector and \mathbf{T}_l as the transformation. Comparing $\mathbf{u}_l = (\mathbf{B}^H \mathbf{R}_x \mathbf{B})^{-1} \mathbf{B}^H \mathbf{R}_x \mathbf{c}_{1,l}$ in (43) with (16), and using $\mathbf{B}_l = \mathbf{B} \mathbf{T}_l$, it is straightforward to see that a reduced size blocking matrix can be chosen as

$$\begin{aligned} \mathbf{B}_l &= \mathbf{B} \left[\mathbf{B}^H \mathbf{R}_x \mathbf{c}_{1,l}, (\mathbf{B}^H \mathbf{R}_x \mathbf{B}) \mathbf{B}^H \mathbf{R}_x \mathbf{c}_{1,l}, \mathbf{K}, (\mathbf{B}^H \mathbf{R}_x \mathbf{B})^{(P-1)} \mathbf{B}^H \mathbf{R}_x \mathbf{c}_{1,l} \right] \\ &= \left[\mathbf{B} \mathbf{B}^H \mathbf{R}_x \mathbf{c}_{1,l}, (\mathbf{B} \mathbf{B}^H \mathbf{R}_x)^2 \mathbf{c}_{1,l}, \mathbf{K}, (\mathbf{B} \mathbf{B}^H \mathbf{R}_x)^P \mathbf{c}_{1,l} \right] \end{aligned} \quad (45)$$

The computation of adaptive weight vectors in (43) requires a matrix inversion, which may be a demanding task even the reduced size \mathbf{B}_l is used in place of \mathbf{B} . In order to avoid such computation, a scheme is proposed based on a decorrelating (Gram-Schmidt) process that is applied to reconstruct $\mathbf{B}_l = [\mathbf{b}_{l,1}, \mathbf{L}, \mathbf{b}_{l,P}]$:

1. Initialization: $\mathbf{P}_0^\perp = \mathbf{B} \mathbf{B}^H$ and
2. For $p = 1, \mathbf{K}, P$

$$\begin{aligned} \tilde{\mathbf{b}}_{p,l} &= \mathbf{P}_{p-1}^\perp \left(\mathbf{B} \mathbf{B}^H \mathbf{R}_x \right)^P \mathbf{c}_{1,l} \\ \mathbf{P}_p^\perp &= \mathbf{P}_{p-1}^\perp - \frac{\mathbf{b}_{l,p} \mathbf{b}_{l,p}^H}{\mathbf{b}_{l,p}^H \mathbf{b}_{l,p}} \end{aligned}$$

An interesting observation gleaned from the above procedure is that $\mathbf{b}_{l,i}^H \mathbf{R}_x \mathbf{b}_{l,j} = 0$ for $|i-j| > 1$, i.e., $\mathbf{B}_l^H \mathbf{R}_x \mathbf{B}_l$ has a symmetric tri-diagonal structure. The following procedure then “diagonalizes” $\mathbf{B}_l^H \mathbf{R}_x \mathbf{B}_l$ by decorrelating $\mathbf{b}_{l,i}$ and $\mathbf{b}_{l,j}$ for $|i-j| > 1$:

$$\begin{aligned} \tilde{\mathbf{u}}_{p,l} &= \frac{\mathbf{b}_{l,p}^H \mathbf{R}_x \mathbf{b}_{l,p-1}}{\mathbf{b}_{l,p}^H \mathbf{R}_x \mathbf{b}_{l,p}} \\ \mathbf{b}_{l,p-1} &= \mathbf{b}_{l,p-1} - \tilde{\mathbf{u}}_{p,l} \mathbf{b}_{l,p} \end{aligned}$$

for $p = P, \mathbf{K}, 1$. The columns of \mathbf{B}_l satisfy the \mathbf{R}_x -conjugacy property [16], i.e.:

$$\mathbf{b}_{l,r}^H \mathbf{R}_x \mathbf{b}_{l,s} = E \left\{ \mathbf{b}_{l,r}^H \mathbf{x}(i) \left(\mathbf{b}_{l,s}^H \mathbf{x}(i) \right)^* \right\} = 0 \quad (46)$$

for $r \neq s$. It follows that the outputs from different columns of \mathbf{B}_l are uncorrelated with

each other. This leads to a significant simplification in the computation of GSC weight vector in (49). Replacing \mathbf{B} in (43) by \mathbf{B}_l , we have

$$\mathbf{w}_l = \left[\mathbf{I} - \left(\sum_{p=1}^K d_p \mathbf{b}_{l,p} \mathbf{b}_{l,p}^H \right) \mathbf{R}_x \right] \mathbf{c}_{1,l} \quad (47)$$

where $d_p = \left(\mathbf{b}_{l,p}^H \mathbf{R}_x \mathbf{b}_{l,p} \right)^{-1}$. The new GSC weight vector based on \mathbf{B}_l involves no matrix inversion as desired.

3.3.3 Partially Adaptive Implementation Based on Conjugate Gradient Method

The receiver output with can be express as

$$\begin{aligned} \bar{z}_{1,l}(i) &= \mathbf{c}_{1,l}^H \mathbf{x}(i) \\ &= \mathbf{c}_{1,l} \mathbf{h}_1 d_1(i) + \mathbf{c}_{1,l}^H \sum_{k=2}^K \mathbf{h}_k d_k(i) + \mathbf{c}_{1,l}^H \mathbf{n}(i) \\ &= \kappa_1 d_1(i) + \sum_{k=2}^K \kappa_k d_k(i) + \mathbf{c}_{1,l}^H \mathbf{n}(i) \end{aligned} \quad (48)$$

where $\kappa_1 = \mathbf{c}_{1,l}^H \mathbf{h}_1$ and $\kappa_k = \mathbf{c}_{1,l}^H \mathbf{h}_k$ are scalar. Then the cross-correlation of input and output in the upper branch of GSC is obtained

$$\begin{aligned} \mathbf{R}_x \mathbf{c}_{1,l} &= E \left\{ \mathbf{x}(i) \left(\mathbf{c}_{1,l}^H \mathbf{x}(i) \right)^H \right\} \\ &= E \left\{ d_1(i) \left(\bar{z}_{1,l}(i) \right)^H \right\} \mathbf{h}_1 + \sum_{k=2}^K E \left\{ d_k(i) \left(\bar{z}_{1,l}(i) \right)^H \right\} \mathbf{h}_k + E \left\{ \mathbf{n}(i) \left(\bar{z}_{1,l}(i) \right)^H \right\} \end{aligned} \quad (49)$$

From (49), we make the following observation: The $\mathbf{R}_x \mathbf{c}_{1,l}$ contain the complete composite MAI's vector. Then, the maximum effectively composite MAI's vector, $\bar{\mathbf{i}}$, should be estimated by projection to the null space of \mathbf{C}_1 :

$$\begin{aligned} \bar{\mathbf{i}} &= \mathbf{B} \mathbf{B}^H \mathbf{R}_x \mathbf{c}_{1,l} \\ &\approx \mathbf{B} \mathbf{B}^H \left(\sum_{k=2}^K E \left\{ d_k(i) \left(\bar{z}_{1,l}(i) \right)^H \right\} \mathbf{h}_k \right) \end{aligned} \quad (50)$$

where we assume orthogonal columns of \mathbf{B} such that $\mathbf{B}^H \mathbf{B} = \mathbf{I}$. Next, according to the GSC scheme in (42), the purpose of lower branch is found \mathbf{u}_l such that performs a mutual cancellation of the of MAI between the upper and lower branches

$$\mathbf{B} \mathbf{B}^H \mathbf{R}_x \mathbf{B} \mathbf{u}_l = \bar{\mathbf{i}}_l \quad (51)$$

Given the maximum effectively composite MAIs vector, a reduced size blocking matrix $\mathbf{B}_{l,p}$, for $l=1,K,L$, retaining the maximum MAI can be constructed by P ($P < N_r(M-1) + L(N_r-1)$) steps CG algorithm. The CG algorithm is an iterative methods in order to solve a system $\overline{\mathbf{R}}\mathbf{w}_l = \overline{\mathbf{i}}_l$ where $\overline{\mathbf{R}}$ is assumed to be Hermitian and positive definite. If an optimal solution \mathbf{w}_l exists, it is obtained after P steps, thus, $\overline{\mathbf{w}}_l = \mathbf{w}_l^{(P)}$. The following is the implementation of PA GSC of CG algorithm [16] in P steps in which $\overline{\mathbf{R}} = \mathbf{B}\mathbf{B}^H\mathbf{R}_x$ and $\overline{\mathbf{i}}_l = \mathbf{B}\mathbf{B}^H\mathbf{R}_x\mathbf{c}_{1,l}$.

1. Initialization: $\mathbf{r}_{l,0} = \mathbf{B}\mathbf{B}^H\mathbf{R}_x\mathbf{B}\mathbf{u}_l$ and $\mathbf{w}_l^{(0)} = 0$

2. Iteration:

for $p = 1$ to P do

if $p = 1$

$$\mathbf{b}_{l,1} = \mathbf{r}_{l,0}$$

else

$$\beta_{l,p} = \frac{\mathbf{r}_{l,p-1}^H \mathbf{r}_{l,p-1}}{\mathbf{r}_{l,p-2}^H \mathbf{r}_{l,p-2}}$$

$$\mathbf{b}_{l,p} = \mathbf{r}_{l,p-1} + \beta_{l,p} \mathbf{b}_{l,p-1}$$

end if

$$\alpha_{l,p} = \frac{\mathbf{r}_{l,p-1}^H \mathbf{r}_{l,p-1}}{\mathbf{b}_{l,p}^H \overline{\mathbf{R}} \mathbf{b}_{l,p}}$$

$$\mathbf{w}_l^{(p)} = \mathbf{w}_l^{(p-1)} + \alpha_{l,p} \mathbf{b}_{l,p}$$

$$\mathbf{r}_{l,p} = \mathbf{r}_{l,p-1} - \alpha_{l,p} \overline{\mathbf{R}} \mathbf{b}_{l,p}$$

end for

3. Approximate solution at P steps:

$$\overline{\mathbf{w}}_l = \mathbf{w}_l^{(P)}$$

In the algorithm, the $\mathbf{b}_{l,p}$ is the search direction at iteration step p and ensure its $\overline{\mathbf{R}}$ -conjugacy to any other vector $\mathbf{b}_{l,q}$, $q \neq p$, i.e.

$$\mathbf{b}_{l,p}^H \overline{\mathbf{R}} \mathbf{b}_{l,q} = 0 \quad \forall q \neq p \quad (52)$$

for $l=1,K,L$ and $p=1,K,P$. After P steps iteration, we can construct the PA blocking matrix $\mathbf{B}_{l,p}$:

$$\mathbf{B}_l = [\mathbf{b}_{l,1} \ \dots \ \mathbf{b}_{l,P}] \quad (53)$$

whose columns form an orthonormal basis and $\overline{\mathbf{R}}$ -conjugacy. Simple algebra shows that \mathbf{B}_l is an $N_r(M+L-1) \times P$ matrix which removes the signal and retains as much MAI as possible in the sense of maximum interference projection. Moreover, the fact that the low branch signals are “ $\overline{\mathbf{R}}$ -conjugacy” facilitates a simple realization of the GSC in which the P adaptive weights are determined individually via the MMSE criterion:

$$\min_{v_{l,p}} E \left\{ \left| \mathbf{c}_{1,l}^H \mathbf{x}(i) - v_{l,p}^* \mathbf{b}_{l,p}^H \mathbf{x}(i) \right|^2 \right\} \quad (54)$$

for $l=1, \dots, L$ and $p=1, \dots, P$. The solution is

$$v_{l,p} = \frac{\mathbf{b}_{l,p}^H \mathbf{R}_x \mathbf{c}_{1,l}}{\mathbf{b}_{l,p}^H \mathbf{R}_x \mathbf{b}_{l,p}} \quad (55)$$

On the other hand, the solution $\overline{\mathbf{w}}_l = \mathbf{w}_l^{(P)}$ of the system $\overline{\mathbf{R}} \mathbf{w}_l = \overline{\mathbf{i}}_l$ lies in the subspace of the basis of the PA blocking matrix $\mathbf{B}_{l,P}$. Then, the relation $\overline{\mathbf{w}}_l$ with $\mathbf{B}_{l,P} \mathbf{v}_l$ is given

$$\overline{\mathbf{w}}_l \propto \mathbf{B}_{l,P} \mathbf{v}_l \quad (56)$$

where $\mathbf{v}_l = [v_{l,1}, \dots, v_{l,P}]^T$. Furthermore, we can find the scalar adaptive weights via the MMSE criterion in (54) similarly

$$v_{l,p} = \frac{\mathbf{b}_{l,p}^H \mathbf{R}_x \mathbf{c}_{1,l}}{\mathbf{b}_{l,p}^H \mathbf{R}_x \mathbf{b}_{l,p}} \quad (57)$$

The overall weight vectors of the proposed GSC receiver can be expressed as

$$\begin{aligned} \mathbf{w}_l &= \mathbf{c}_{1,l} - \mathbf{B}_{l,P} \mathbf{v}_l \\ &= \mathbf{c}_{1,l} - \overline{\mathbf{w}}_l \mathbf{v}_l \end{aligned} \quad (58)$$

3.3.4 RAKE Combining and Decision Aided Symbol Detection

With the adaptive correlator bank constructed, the next step is to perform a maximum ratio combining of the correlator outputs to collect the multipath energy. Since the MAI has been removed, channel estimation (i.e., $\alpha_{1,l}^{(j)}$'s) for the desired user can be done accurately, leading to improved performance as compared to the conventional RAKE receiver. However, the GSC is blind in nature and usually exhibits slow convergence due to the residual signal effect [17]. To remedy this, an iterative decision aided scheme is introduced in which the

signal is estimated and then subtracted from the input data before the computation of GSC adaptive weights.

First, assume that at the j th iteration, the received data $\mathbf{x}(i)$ is despread at the L fingers into:

$$\mathcal{S}_{1,l}^{(j)}(i) = \mathbf{w}_l^{(j)H} \mathbf{x}(i) \quad (59)$$

for $l=1, K, L$, where $\mathbf{w}_l^{(j)}$ is obtained by (58) using the "signal-subtracted" data vector $\mathbf{y}^{(j)}(i)$ as the GSC input:

$$\mathbf{y}^{(j)}(i) = \mathbf{x}(i) - \mathcal{S}_1^{(j-1)}(i) \quad (60)$$

with $\mathcal{S}_1^{(j-1)}(i)$ being the desired signal estimated at the $(j-1)$ th iteration ($\mathcal{S}_1^{(0)}(i) = \mathbf{0}$). That is, the correlation matrix \mathbf{R}_x in (58) is replaced by $\mathbf{R}_{ij}^{(j)} = E\{\mathbf{y}^{(j)}(i)\mathbf{y}^{(j)}(i)^H\}$. After filtering, the channel gain estimates at the L fingers can be obtained using a sequence of N_p pilot symbols:

$$\alpha_{1,l}^{(j)} = \frac{1}{N_r M N_p} \sum_{i=1}^{N_p} \mathcal{S}_{1,l}^{(j)}(i) d_1^*(i) \quad (61)$$

for $l=1, K, L$, where M is the normalizing factor accounting for the processing gain. Note that $\alpha_{1,l}^{(j)}$ includes the effect of transmit power σ_1^2 . Using these channel estimates, a coherent RAKE combining of $\mathcal{S}_{1,l}^{(j)}(i)$'s is achieved by

$$\mathcal{S}_1^{(j)}(i) = \sum_{l=1}^L \alpha_{1,l}^{(j)*} \mathcal{S}_{1,l}^{(j)}(i) \quad (62)$$

which is then sent to the data decision device:

$$\mathcal{A}_1^{(j)}(i) = \text{dec}\{\mathcal{S}_1^{(j)}(i)\} \quad (63)$$

Second, signal reconstruction is done by exploiting the channel estimates $\alpha_{1,l}^{(j)}$'s, the desired user's signature $\mathbf{c}_{1,l}$ and symbol decisions $\mathcal{A}_1^{(j)}(i)$ and is expressed as

$$\mathcal{S}_1^{(j)}(i) = \left(\sum_{l=1}^L \alpha_{1,l}^{(j)} \mathbf{c}_{1,l} \right) \mathcal{A}_1^{(j)}(i) \quad (64)$$

Note that $\alpha_{1,l}^{(j)}$'s are used for both signal reconstruction and symbol detection. Finally, the reconstructed signal is subtracted from the data sent to the $(j+1)$ th iteration, which yields

$$\mathbf{y}^{(j+1)}(i) = \mathbf{x}(i) - \mathcal{S}_1^{(j)}(i) \quad (65)$$

By using $\mathbf{y}^{(j+1)}(i)$ as the GSC input, the adverse slow convergence can be effectively improved, and the PA CDMA multi-user receiver can achieve its optimal performance with a moderate size of data samples. Due to signal subtraction, the receiver will act like the optimal MSINR receiver operating on \mathbf{R}_{in} , which offers the best compromise between MAI plus noise suppression and signal reception. The above steps can be iterated $J>2$ times, if necessary.

3.4 Extended Research Achievement

It is widely accepted that the combination of smart antenna and MUD techniques leads to the MIMO era. In the future, it is thus natural for us to aim at the MIMO technologies for in-depth study based on our research results, including diversity and BLAST algorithms. In this project, we propose an MIMO MC-CDMA (multicarrier-CDMA) transmission architecture to enhance the system performance, e.g., link quality and data rate, by increasing the spatial and temporal degrees of freedom. In addition, the proposed system can dynamically allocate spreading codes according to users' data rate requirement, and BLAST processors detect each user's signal at receive end. The proposed MC-CDMA transmission architecture is shown as figure 5.

4. Simulation Results

Simulation 1-Linear Space-Time RAKE Receiver: Here we evaluate the performance of the proposed ST receiver using a linear array of $N_r = 4$ identical elements uniformly spaced by a $1/2$ wavelength. The inter-antenna spacing is chosen specifically for the field-of-view $[-60^\circ, 60^\circ]$. For all users, $L = 3$ paths are generated with the delays $\tau_{k,l}$'s chosen from. It is assumed that the three paths of the signal-of-interest arrived from -20° , 0° and 20° , respectively, and those of the MAI are randomly distributed in the entire field-of-view. All CDMA signals are generated with BPSK data modulation and spread with the Gold code of length $M=31$. In addition to the MAI, there are two equal power BPSK NBI's arriving from 40° and -40° , respectively, which are chosen to be well separated from the signal-of-interest. The NBI bit rate is 0.8 times that of the CDMA signals such that the NBI will appear to be time-varying interference to the receiver [10]. For each result, $N_s = 500$ symbols (including pilot symbols) are used to estimate the correlation matrices, and a total of 1000 Monte-Carlo runs are executed. In direct matrix inversion weight vector computation, the pseudo noise power μ_u is chosen to be one fifth of the largest eigenvalue of $\mathbf{R}_x^{(n_r)}$. As a performance index, the output SINR is defined as

$$\text{SINR}_o = 10 \log_{10} \frac{\text{output power of signal in } z_1(i)}{\text{output power of (MAI+NBI+noise) in } z_1(i)}$$

and the input SNR (SNR_i) is defined as the ratio of the signal power to noise power. The NFR is the ratio of the MAI power to signal power before despreading, and the NBI-to-signal-ratio (NSR) is the ratio of the NBI power to signal power before despreading. The BER is measured for each case with a total of $500 \times 1000 = 500000$ symbols after the adaptive weights are obtained. For comparison, we also included the results obtained with the ST-MMSE receiver using different numbers of training symbols. The ST-MMSE receiver is derived based on (16). In the first three simulations, both receivers are evaluated in the batch mode. In the 500 received symbols, $N_p = 50$ pilot symbols are used for the proposed receiver, but different numbers of pilot symbols $N_p = 50, 250, 450$ are used for the ST-MMSE receiver.

In the first simulation, the patterns of diversity beams of the proposed ST receiver for the 1st, 2nd and 3rd paths are plotted for the case $K=5$ users, $\text{NFR}=0$ dB, $\text{SNR}_i=0$ dB and

NSR=20 dB. As shown in Figure 6, the mainlobes and deep nulls confirm that the adaptive beamformers can effectively collect the desired signals and suppress the NBI.

In the second simulation, the system performance is evaluated in Figure 7 for ST-MMSE and proposed ST receivers, with NFR=0 dB, SNR_i=0 dB and NSR=20 dB. Figure 7 shows the output SINR results. As expected, the ST-MMSE receiver gives the best performance with a long training sequence, in which both channel estimation and MAI/NBI suppression can be done effectively. A trade-off for this, however, is the decrease in system efficiency. On the other hand, the proposed ST receiver gives better performance than the ST-MMSE receiver with $N_p = 50, 250$, indicating that the adaptive filters and beamformers have successfully eliminated the MAI and strong NBI. The ST-MMSE receiver weight vector has a large size of $34 \times 4 = 136$, and this is the reason why it requires a long training sequence for convergence.

In the third simulation, the near-far resistance of ST-MMSE and proposed ST receivers are evaluated with different NFR values. Figures 8 show the output SINR obtained with $K=5$, SNR_i=0 dB and NSR=20 dB. It is observed that the ST-MMSE receiver performs poorly with $N_p = 50$ and 250 due to the lack of training sequence for strong MAI/NBI suppression. On the contrary, the proposed ST receiver achieves its excellent near-far resistance by successfully canceling the MAI using the temporal degree-of-freedom, and canceling the strong NBI using the spatial degree-of-freedom. In the fourth set of simulations, we show the output SINR and BER results obtained with different input SNR for ST-MMSE and proposed ST receivers, with $K=5$, NFR=20 dB, NSR=20 dB. From Figures 9, we know that the proposed ST receiver again gives an excellent performance.

Finally, to demonstrate the effectiveness of the recursive algorithms of the proposed ST receiver for weight adaptation, we replaced direct matrix inversions by the formulae given in (38) and (39). The adaptation step sizes are chosen as $\mu_u = \mu_w = 10^{-6}$. Figure 10 shows the resulting learning curve obtained with NFR = 0 dB, SNR_i=0 dB, NSR=20 dB and $K=5$. In the 3000 received symbols, $N_p=300$ pilot symbols are used for the proposed receiver, i.e., the pilot-to-data ratio $N_p/N_s=1/10$ is the same as in the first three simulations. The proposed receiver converges in about 200 symbols (including data and pilot symbols), confirming that it can be implemented in the time-recursive fashion to combat the MAI and NBI in a

stationary environment. To show the tracking capability of the algorithm, we repeated the same simulation, but deliberately changed the AOA's of two NBI's from -40° and 40° to 20° and -10° , respectively, at the 500th iteration. In this scenario, the spatial steering vectors of the two NBI's are changed abruptly, and the adaptive beamformers could not respond instantly to suppress the NBI's, leading to a steep drop in the output SINR as shown in Figure 11. However, the learning curve confirms that the recursive receiver (especially the beamformer part) can successfully respond and adjust its weights to environmental changes such as moving NBI.

Simulation 2-Partially Adaptive ST CDMA Receiver: Simulation results are demonstrated to confirm the performance of the proposed PA receiver in a time-multiplexed pilot symbols assisted system. The receiver output SINR is used as the evaluation index. Also, the input SNR is defined as $\text{SNR} = \sigma_1^2 / \sigma_n^2$, and the near-far-ratio is defined as $\text{NFR} = \sigma_k^2 / \sigma_1^2$, $k = 2, \dots, K$, where we assume equal power MAI for convenience. The path gains $\alpha_{n_r, k, l}$'s are assumed independent, identically distributed unit variance complex Gaussian random variables, the path delays $\tau_{k, l}$'s are uniform over $[0, 3T_c]$, and the number of paths is $L=4$. All CDMA signals are generated with BPSK data modulation and Gold codes of length $M=31$ are used as the spreading codes. For each trial, N_s symbols (including data and pilot) are used to obtain the sample estimate of \mathbf{R}_x and \mathbf{R}_y , and N_p pilot symbols are used to obtain $\alpha_{n_r, 1, l}$. Each simulation result is obtained by 200 independent trials, with each trial using a different set of $\alpha_{n_r, k, l}$'s and data/noise sequence. Unless otherwise mentioned, the following parameters are assumed: $K=20$, $\text{SNR}_i = 0$ dB, $\text{NFR} = 20$ dB, $N_s=500$, $N_p=100$, PA dimension $P = \lceil (K-1)/2 \rceil$ and the number of iterations is $J=3$. For comparison, we also include the results obtained with the optimal, MMSE and MOE receivers. The optimal receiver is defined to be the MSINR receiver with \mathbf{R}_{in} obtained by artificially removing $\mathbf{s}_1(i)$ from $\mathbf{x}(i)$ and true CSV \mathbf{h}_1 used. The ST MMSE receiver is given by (16), with \mathbf{H} obtained using N_p pilot symbols. The proposed receiver uses $N_p=N_s/5$ pilot symbols, and the MMSE receiver uses $N_p = N_s$ (full) pilot symbols.

In the first simulation, the output SINR performance versus dimension of blocking matrix of PA receiver is demonstrated. The results given in Figure 12 show that the proposed

PA receiver successively approach the proposed FA receiver at PA dimension $P=7$ and reaches the performance of ST MMSE receiver using full pilot symbols at $P=4$. The simulation results confirm that the proposed PA receiver is able to offer the performance of the FA receiver with a $P = \lceil (K-1)/2 \rceil$ dimensions.

In the fourth simulation, the output SINR performance is evaluated as a function of input SNR. The results shown in Figure 13 indicate that the proposed PA receiver successively approaches the optimal receiver within a wide range of input SNR. In the fifth simulation, the near-far resistance is evaluated with different NFR values. Figure 14 shows the output SINR curves. It is observed that the proposed PA receiver achieves its excellent near-far resistance by successfully canceling the MAI using the temporal degree of freedom offered by the pre-despread data. The system capacity is then evaluated with different values of K . As shown in Figure 15, the proposed PA receiver is able to offer the performance of the optimal receiver in a heavily loaded system with effective MAI suppression using the smallest dimension for adaptive filtering.

Finally, the convergence behavior of the proposed PA receiver is compared with the MMSE receiver. The results given in Figure 16 show that the proposed receiver with 1/5 pilot symbols converges in about $N_s=500$ data symbols. On the other hand, the MMSE receiver using full pilot symbols offers nearly the optimal performance. Again, the reasons for the significant discrepancy between the proposed and MMSE receivers with a low pilot symbol ratio is that the proposed receiver cancels the MAI before channel and frequency offset estimation, whereas the MMSE receiver estimates the channel and frequency offset in the presence of strong MAI.

5. Conclusion

Linear space time RAKE receiver is designed with a three-stage procedure. First, temporal processors are constructed as adaptive filters to suppress MAI. Second, adaptive beamformers are constructed to suppress strong NBI. Finally a simple coherent combiner combines the beamformer outputs to enhance multipath signal reception. From simulation results, it is shown that the proposed receiver is near-far resistant, and performs reliably in an overloaded system, even in the presence of strong NBI, and outperforms the space-time MMSE receiver using the same pilot symbol assisted weight computation.

PA ST CDMA receivers are developed with the following procedure. First, blind adaptive correlators are constructed at different fingers based on the GSC scheme to collect multipath signals and suppress strong interference. For reduced complexity implementation, partial adaptivity is incorporated into the GSC based on the Krylov subspace technique and CG method, leading to an efficient algorithm without the need of matrix inversion. Second, pilot symbols assisted channel estimation and RAKE combining give the estimate of signal symbols. Finally, for further performance enhancement, an iterative decision aided scheme is introduced which reconstructs and subtracts the signal from the GSC input data. This effectively eliminates the performance drop due to finite data samples effect. Simulation study shows that the proposed PA CDMA receiver can achieve nearly the same performance of the optimal MMSE receivers under severe system conditions. The main advantages of the proposed receiver over others lie in a lower implementation complexity and overhead for pilot symbols.

6. References

- [1] S. Verdu, **Multiuser Detection**, Cambridge University Press: New York, 1998.
- [2] G. Woodward and B. S. Vucetic, "Adaptive detection for DS-CDMA," *IEEE proceeding*, vol. 86, pp. 1413-1434, July 1998.
- [3] U. Madhow and M. Honig, "MMSE interference suppression for direct-sequence spread-spectrum CDMA," *IEEE Trans. Commun.*, vol. 42, pp. 3178-3188, Dec. 1994.
- [4] M. Honig, U. Madhow and S. Verdu, "Blind adaptive multiuser detection," *IEEE Trans. Information Theory*, vol. 41, pp. 944-960, July 1995.
- [5] B. D. Van Veen, **Minimum variance beamforming in Adaptive Radar Detection and Estimation**, John Wiley and Sons: NY, 1992.
- [6] H. L. Van Trees, **Optimum Array Processing**, John Wiley and Sons: NY, 2002.
- [7] J. S. Goldstein and I. S. Reed, "Subspace selection for partially adaptive sensor array processing," *IEEE Trans. Aerospace and Electronic Systems*, vol. 33, pp. 539-544, April 1997.
- [8] T. S. Lee, T. C. Tsai and C. H. Chen, "A Beamspace-Time Blind RAKE Receiver for Sectorized CDMA Systems," *Wireless Personal Commun.*, vol. 17, no. 1, pp. 65-83, April 2001.
- [9] T. S. Lee and T. C. Tsai, "A Beamspace-Time Interference Canceling CDMA Receiver for Sectorized Communications in a Multipath Environment," *IEEE JSAC*, vol. 19, no. 7, pp. 1374-1384, July 2001.
- [10] H. V. Poor and X. Wang, "Blind adaptive suppression of narrowband digital interferes," *Wireless Personal Commun.*, vol. 6, pp. 69-96, Feb. 1998.
- [11] H. V. Poor, "Active interference suppression in CDMA overlay systems," *IEEE JSAC*, vol. 19, pp. 4-20, Jan. 2001.
- [12] S. Haykin, **Adaptive Filter Theory**, 3rd ed. New Jersey: Prentice-Hall, 1996.
- [13] T. S. Lee and Z. S. Lin, "A sectorized beamspace adaptive diversity combiner for multipath environments," *IEEE Trans. Veh. Technol.*, vol. 48, pp. 1503-1510, Sep. 1999.
- [14] D. A. Pados and S. N. Batalama, "Low-complexity blind detection of DS/CDMA signals auxiliary-vector receivers," *IEEE Trans. Commun.*, vol. 45, pp. 1586-1594, Dec. 1997.

- [15] C. Wanshi, U. Mitra and P. Schniter, "On the equivalence of three reduced rank linear estimators with applications to DS-CDMA," *IEEE Trans. Commun.*, vol. 48, pp. 2609-2914, Sept. 2002.
- [16] G. Golub and C. V. Loan, **Matrix Computation**, Johns Hopkins University Press, 1996.
- [17] M. Wax and Y. Anu, "Performance analysis of the minimum variance beamformer," *IEEE Trans. Signal Processing*, vol. 44, pp. 928-937, April 1996.

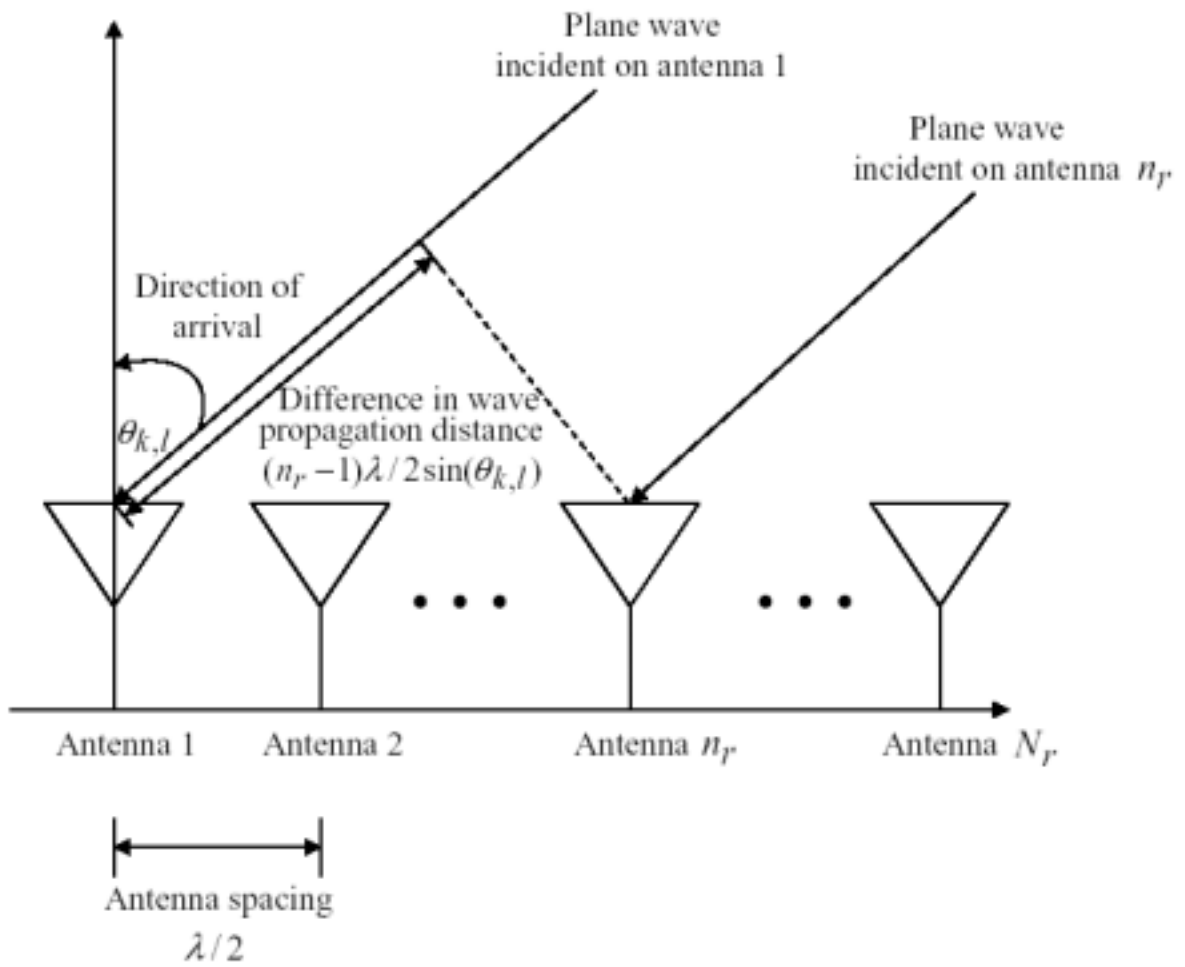


Figure 1: Configuration of linear equally spaced antenna array.

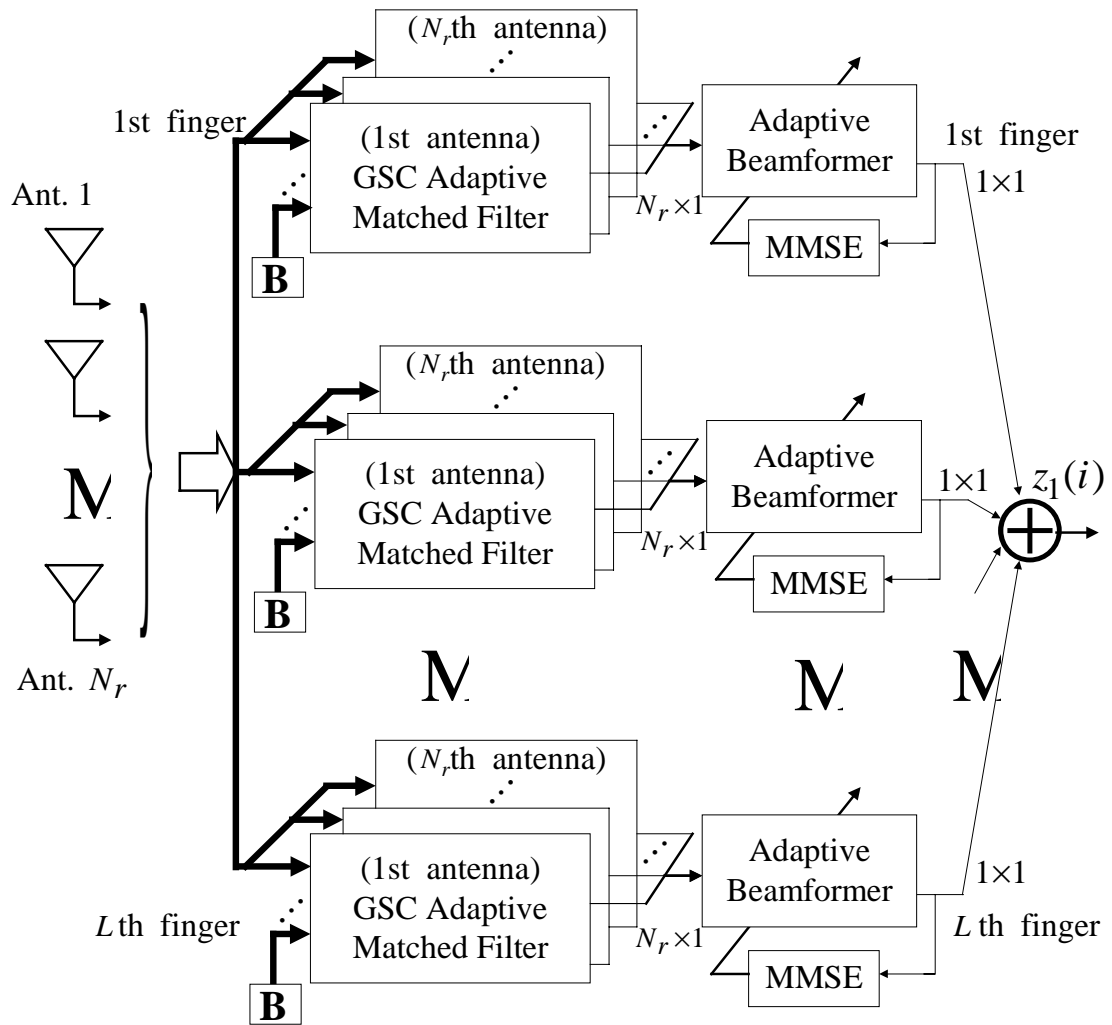


Figure 2: Illustration of proposed ST receiver.

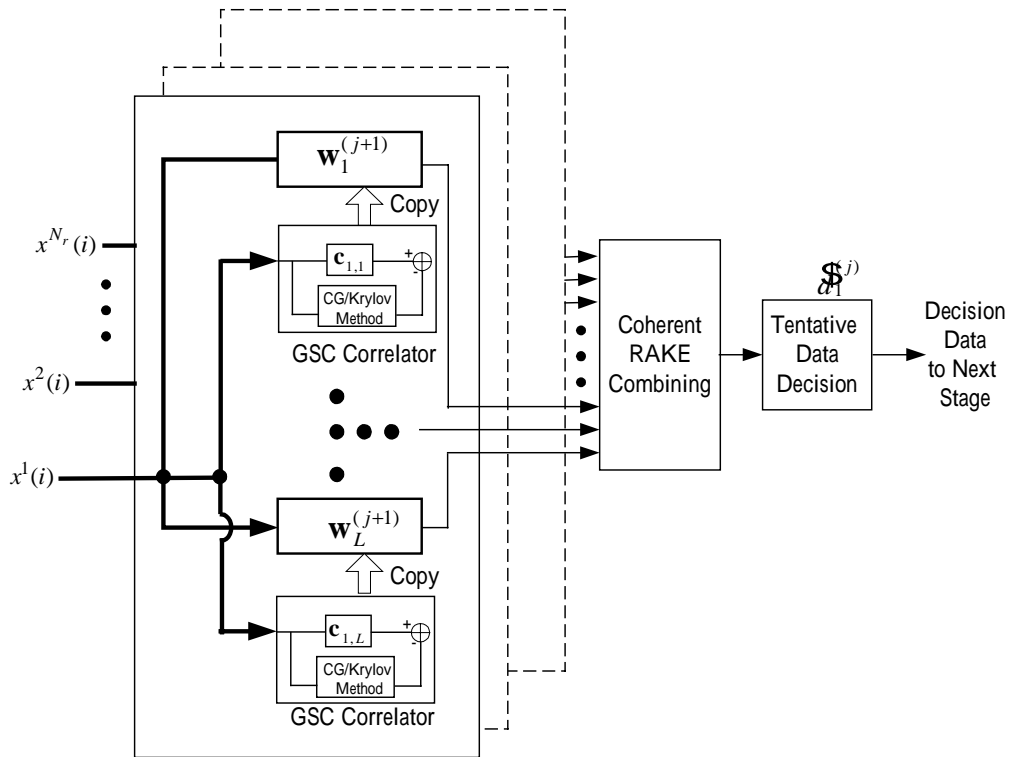


Figure 3: Schematic diagram of proposed ST CDMA receiver with partially adaptive interference cancellation.

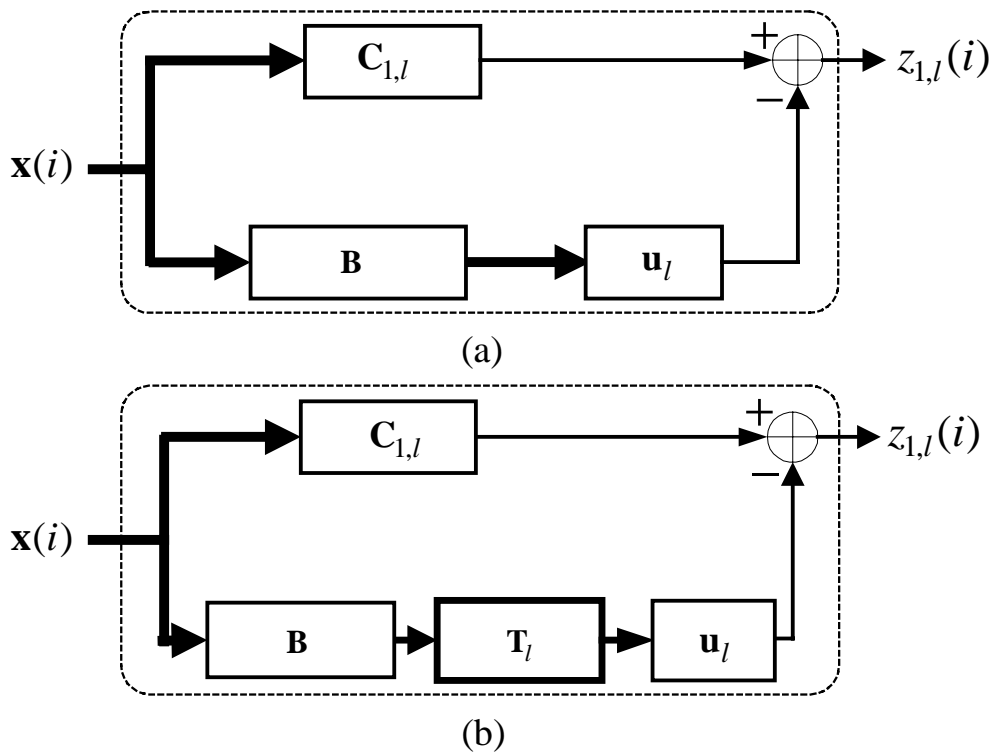
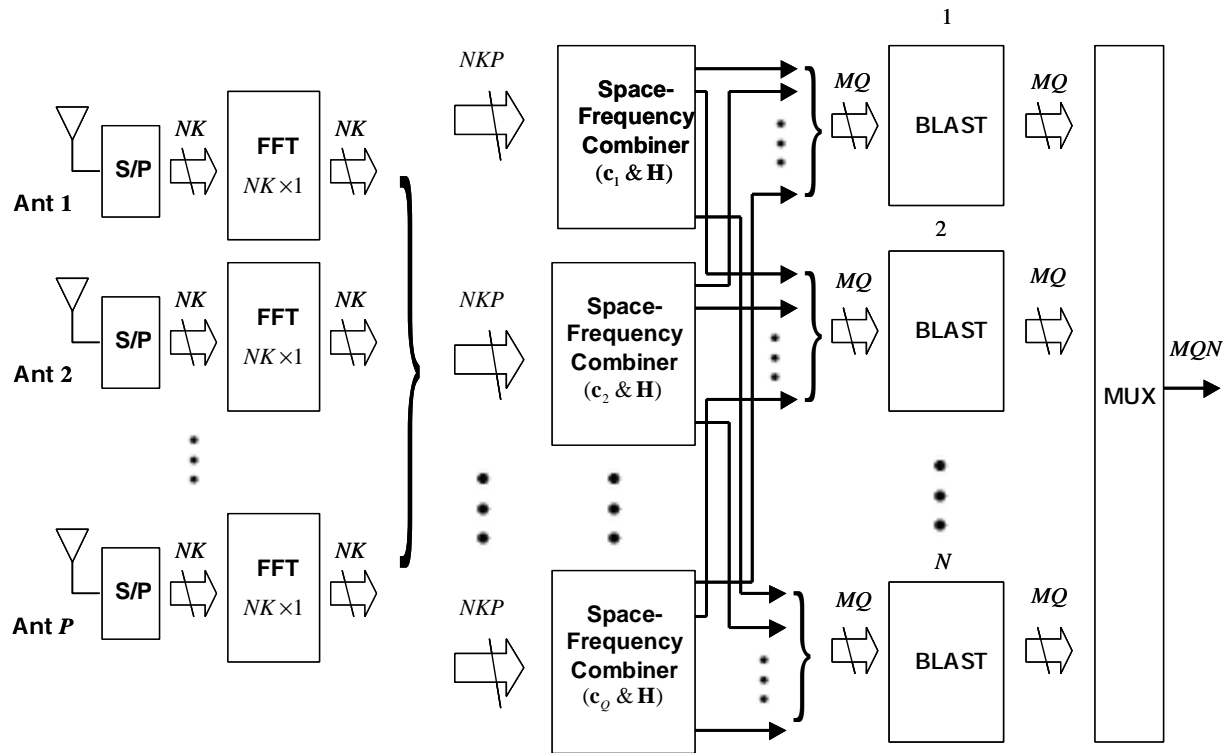
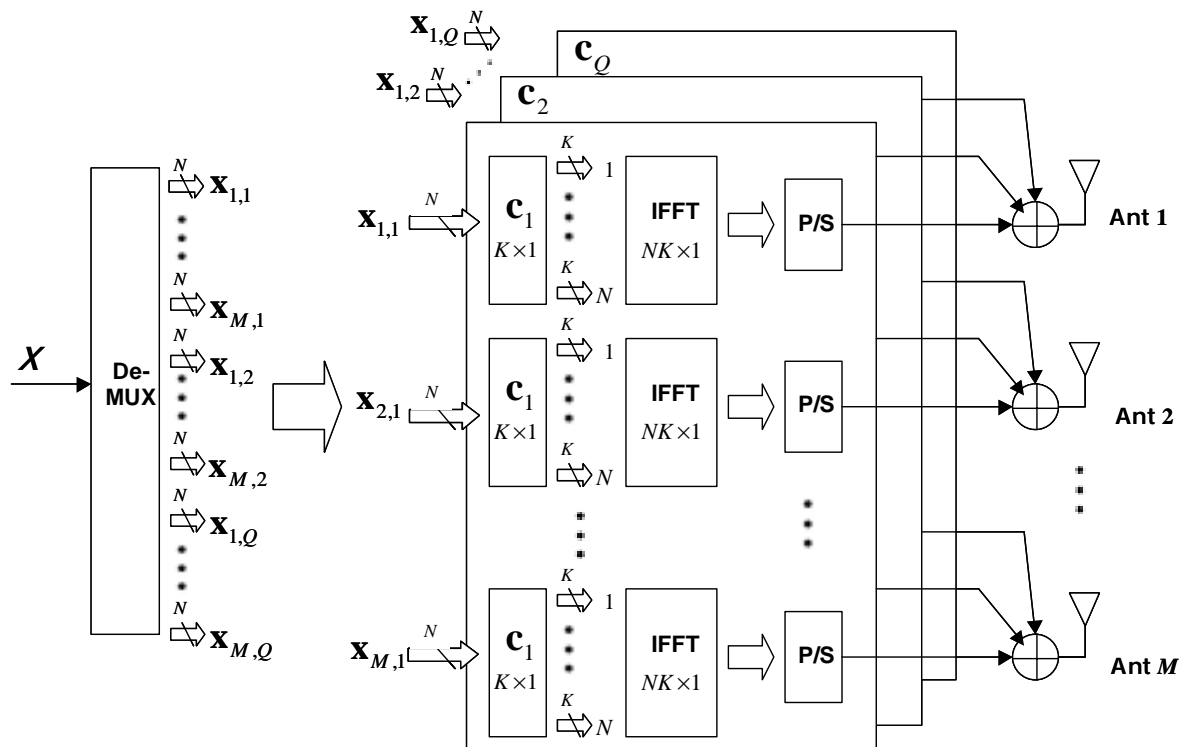


Figure 4: Illustration of (a) fully adaptive GSC (b) partially adaptive GSC.



(a)



(b)

Figure 5: (a) MIMO MC-CDMA transmitter architecture (b) MIMO MC-CDMA receiver architecture.

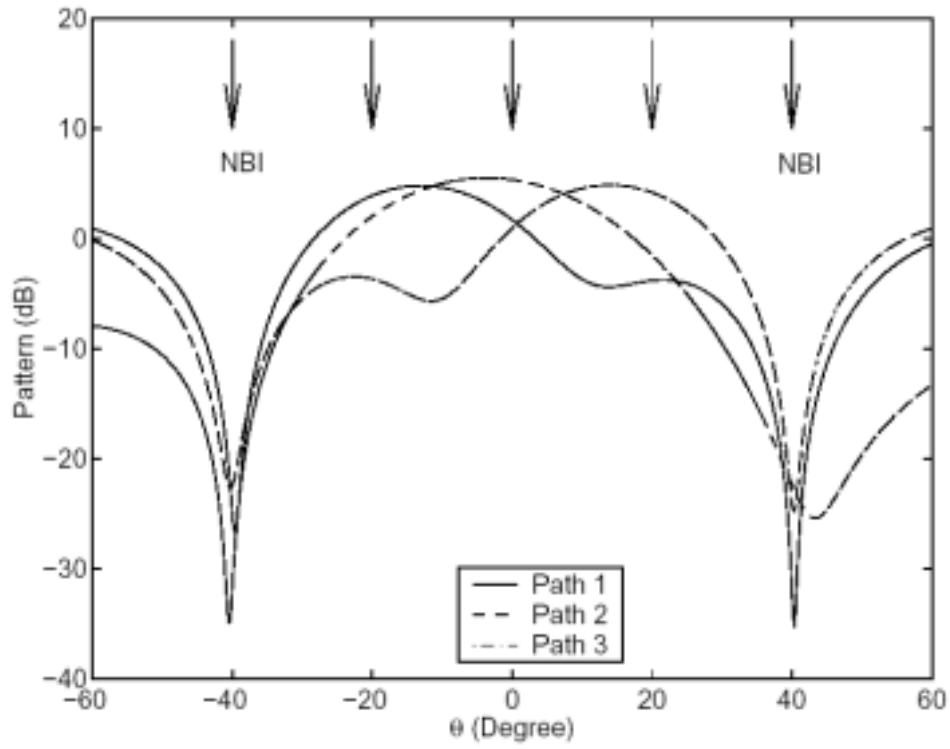


Figure 6: Patterns of diversity beams of the proposed ST receiver obtained with $K=5$, $SNR_i=0$ dB, $NFR=0$ dB and $NSR=20$ dB.

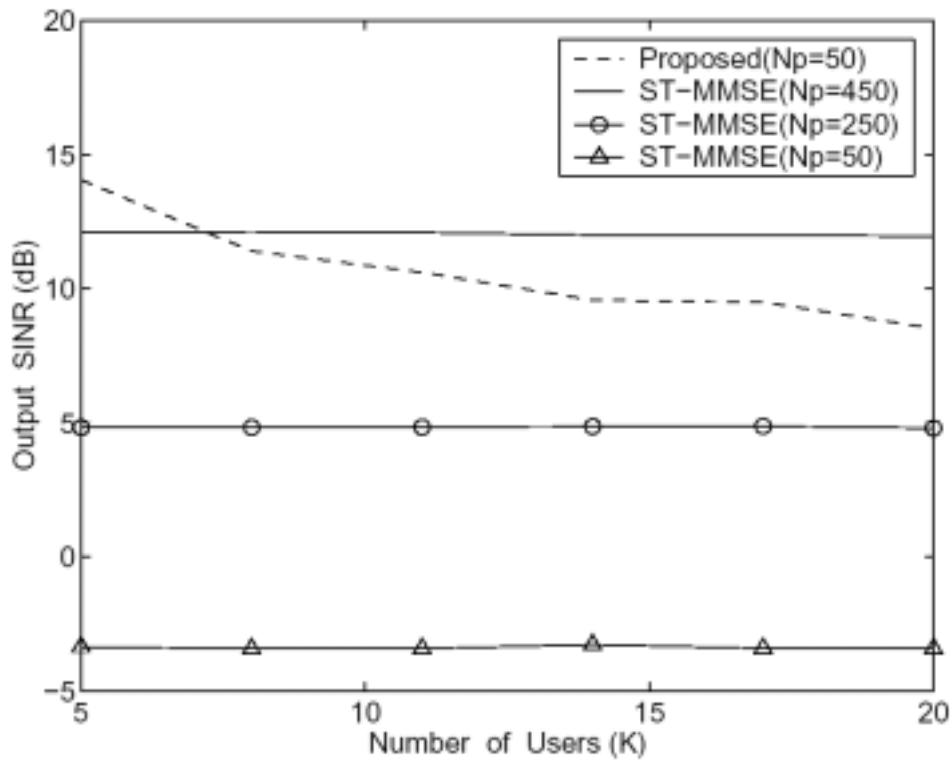


Figure 7: Output SINR versus user number K for ST-MMSE and proposed ST receivers with $SNR_i=0$ dB, $NFR=0$ dB and $NSR=20$ dB.

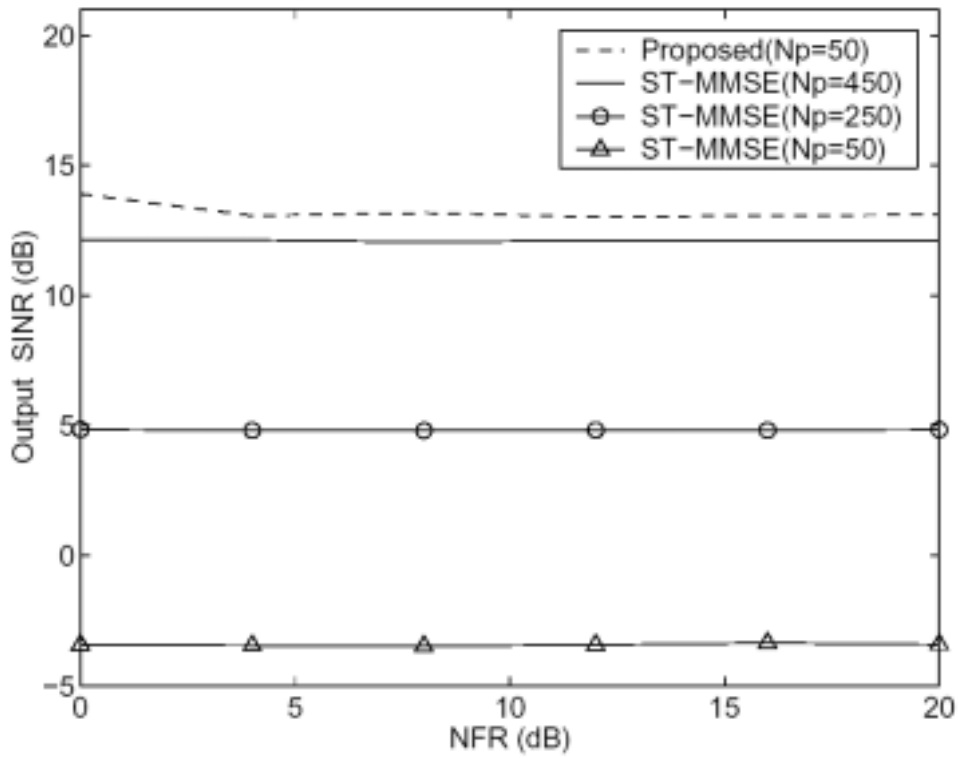


Figure 8: Output SINR versus NFR for ST-MMSE and proposed ST receivers with $K=5$, $SNR_i=0$ dB and $NSR=20$ dB.

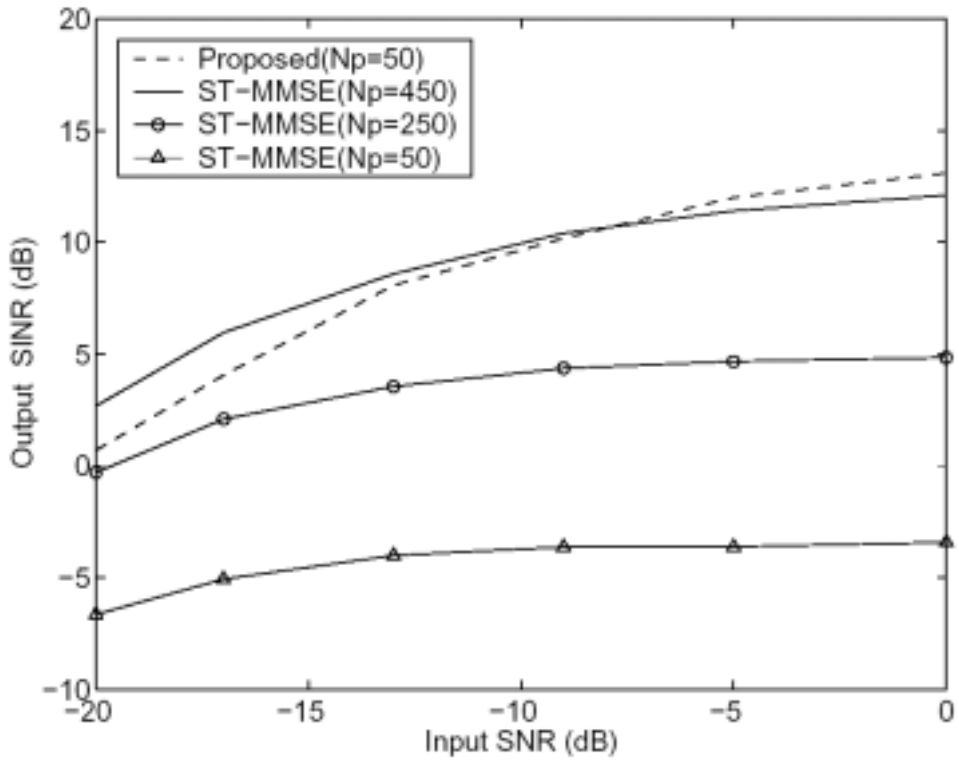


Figure 9: Output SINR versus input SNR for ST-MMSE and proposed ST receivers with $K=5$, $NFR=20$ dB and $NSR=20$ dB.

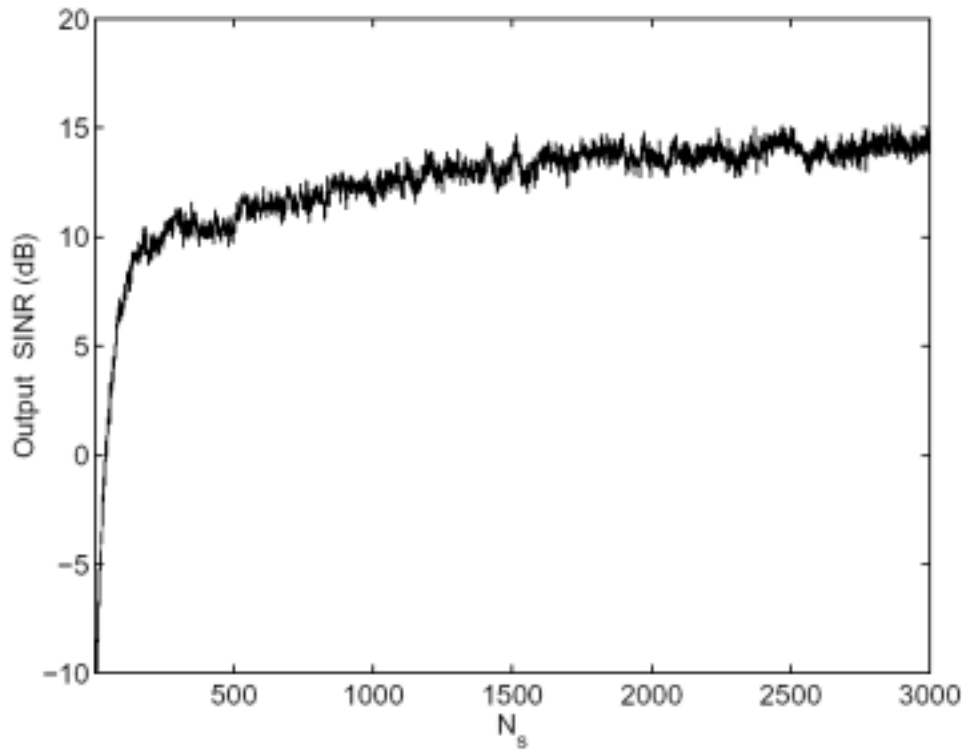


Figure 10: Evaluation of recursive algorithms for proposed ST receiver with $K=5$, $\text{SNR}_i=0$ dB, $\text{NFR}=0$ dB and $\text{NSR}=20$ dB. (NBI's AOA fixed)

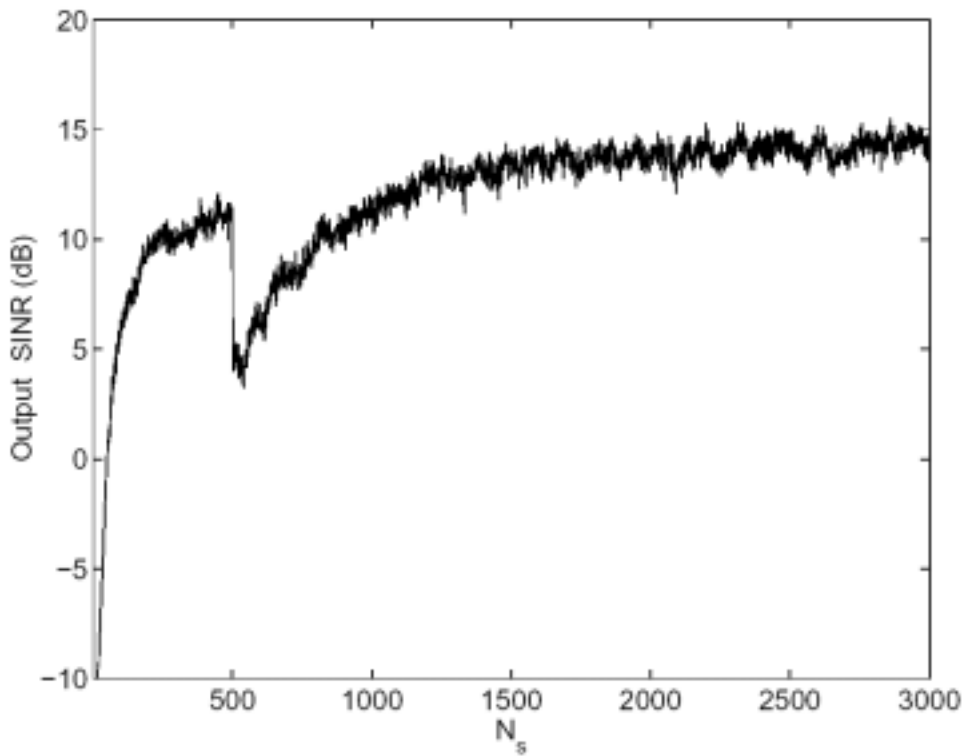


Figure 11: Evaluation of recursive algorithms for proposed ST receiver with $K=5$, $\text{SNR}_i=0$ dB, $\text{NFR}=0$ dB and $\text{NSR}=20$ dB. (NBI's AOA changed at 500th iteration)

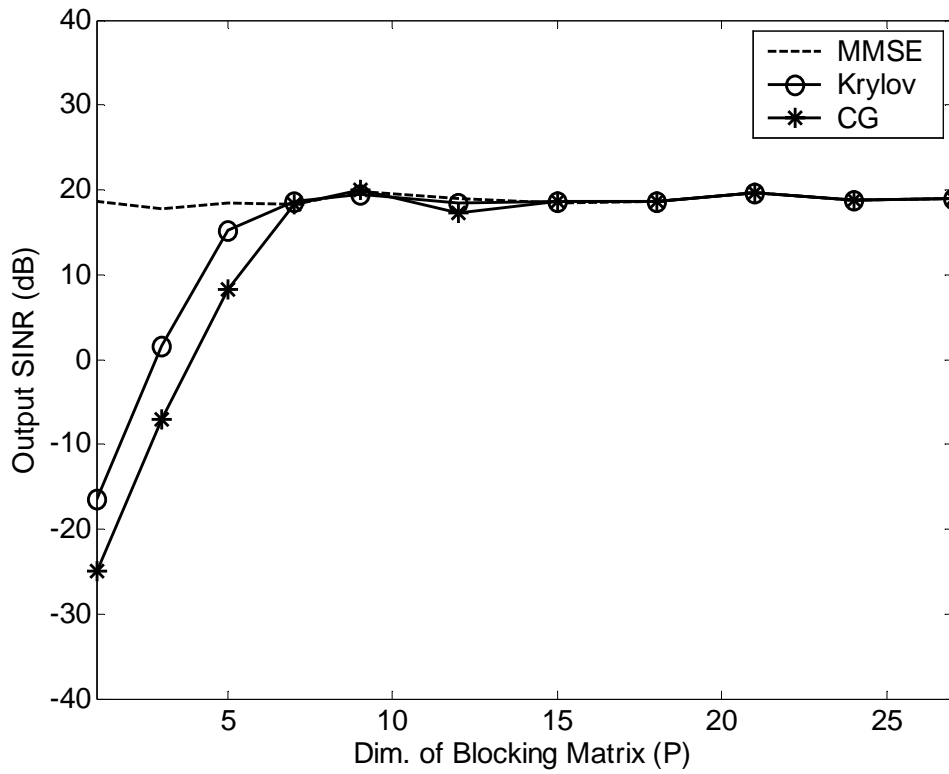


Figure 12: Receiver output SINR versus PA dimension P with $K=20$, $\text{SNR}_i = 0$ dB, $\text{NFR}=20$ dB and $J=3$.

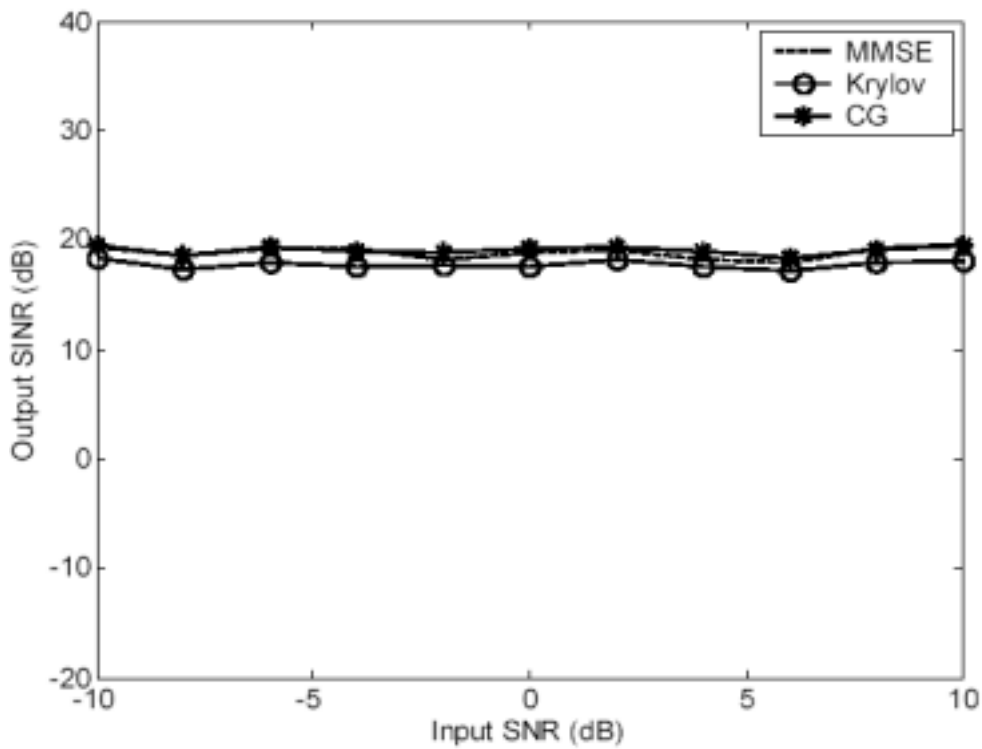


Figure 13: Receiver output SINR versus input SNR with $K=20$, $\text{SNR}_i=0$ dB, $\text{NFR}=20$ dB, $P=10$ and $J=3$.

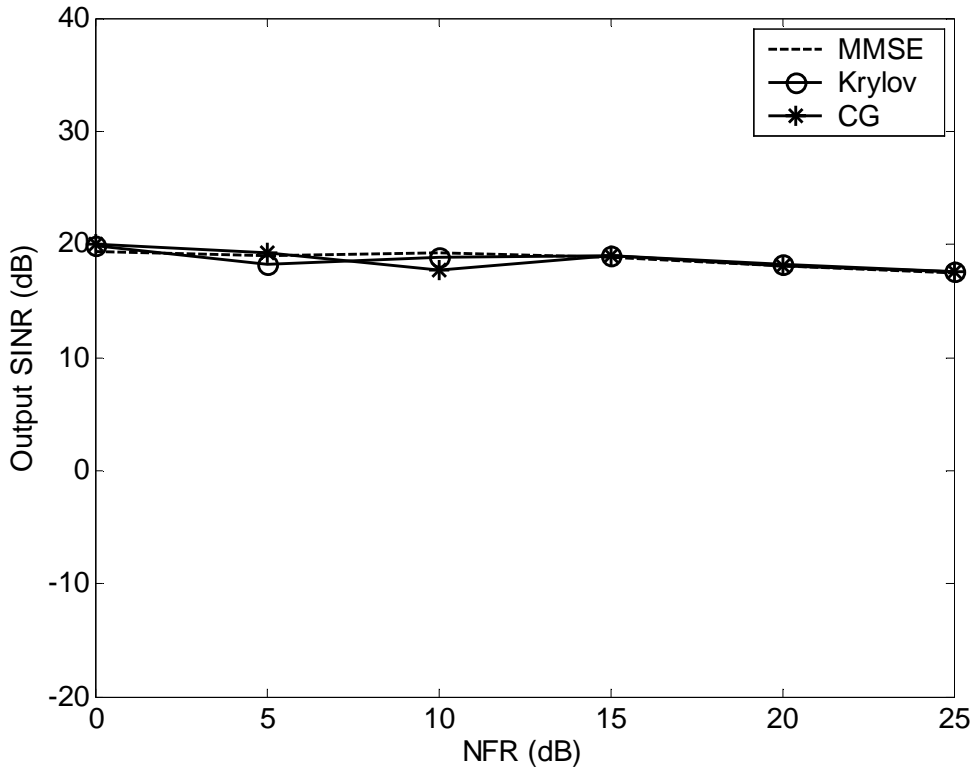


Figure 14: Receiver output SINR versus NFR with $K=20$, $\text{SNR}_i=0$ dB, $P=10$ and $J=3$.

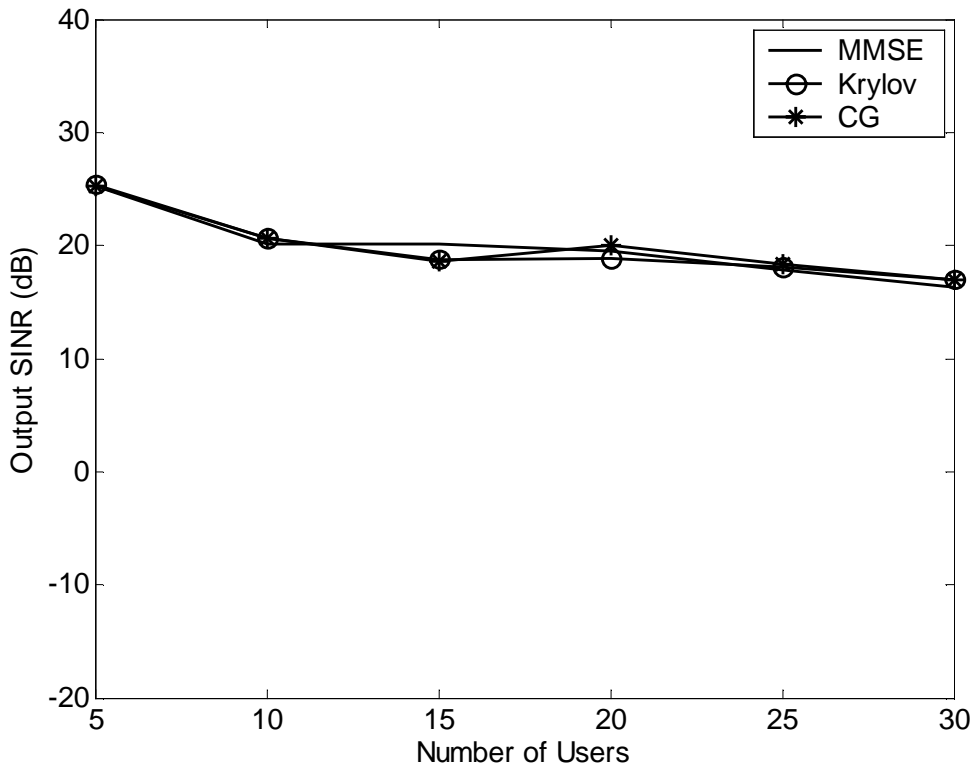


Figure 15: Receiver output SINR versus number of users with $\text{SNR}_i=0$ dB, $\text{NFR}=20$ dB, $P=10$ and $J=3$.

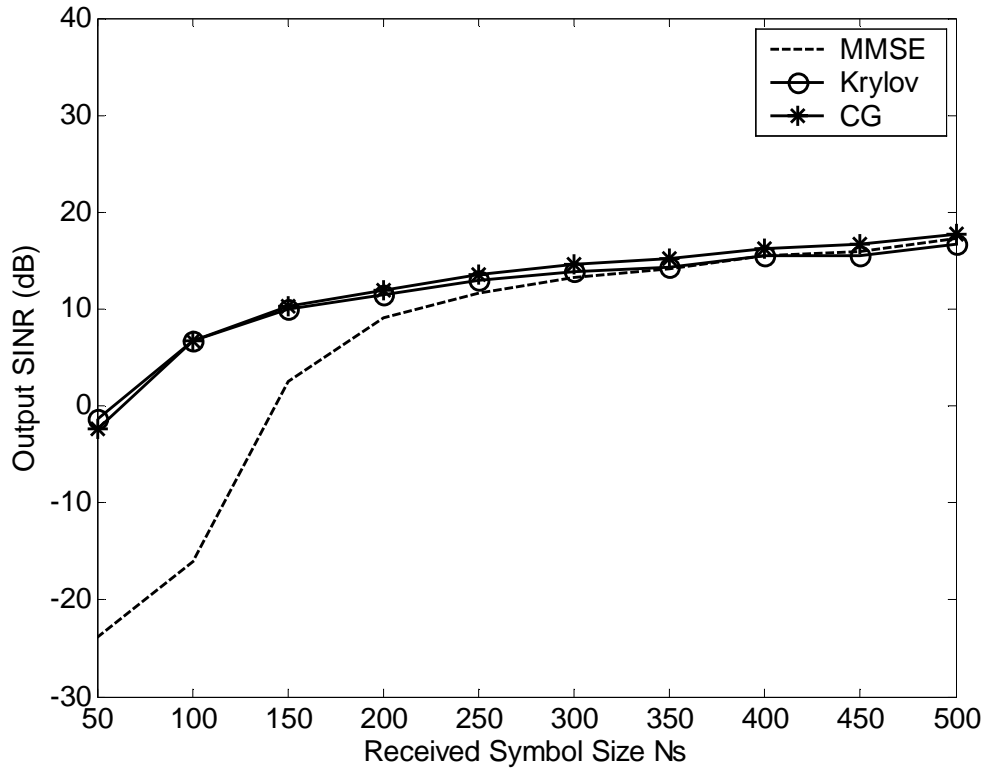


Figure 16: Receiver output SINR versus data sample size N_s with $K=20$, $\text{SNR}_i=0$ dB, $\text{NFR}=20$ dB, $P=10$ and $J=3$.